

An overview on the green synthesis of nanoparticles and other nano-materials using enzymes and their potential applications

Qayyum Husain^{1,*}

¹Department of Biochemistry, Faculty of Life Sciences, AMU Aligarh-202002, India

*corresponding author e-mail address:qayyumbiochem@gmail.com

ABSTRACT

The applications of nanoparticles (NPs) and another nanomaterial (NM) are widely increasing in various fields including biomedical and clinical sciences. Conventional methods used for the synthesis of NM have several demerits like chemical procedures producing toxic materials and physical methods being costly and forming particles of non-uniform sizes. The use of such NM has prevented their applications in biomedical fields especially in clinical applications. In order to use NPs in clinical fields, there is a need to use reliable, nontoxic and eco-friendly methods for their synthesis. The use of eco-friendly and biological methods for the synthesis of NPs and other NM has attracted the attention of nanobiotechnologists due to synthesis of such particles by using nontoxic method. The enzymatic synthesis of NPs is highly specific as this procedure results in the formation of nontoxic materials of controlled shape, size and high stability. In this chapter an effort has been made to critically review recent developments in the area of biosynthesis of several types of NM by using enzymes of diverse groups such as oxidoreductases, transferases, hydrolases, lyases and ligases. The mechanisms of enzyme catalyzed synthesis of NPs and the reaction conditions to control their shape, size, and stability of NPs have also been described. Numerous kinds of techniques employed for the identification and characterization of NM have been discussed. The biomedical and other applications of as-synthesized NM have also been mentioned in this article.

Keywords: *Nanoparticles, nanomaterial, enzymatic synthesis, nanocrystals, nanocomposites, nanobiotechnology.*

Abbreviations: AFM, atomic force microscopy; DLS, dynamics light scattering; EDX, energy dispersive X-ray; FT-IR, fourier transform infrared; GO, graphite oxide; GOD, glucose oxidase; GR, glutathione reductase; GS, glutathione synthetase; HRP, horseradish peroxidase; HRTEM, high resolution-transmission electron microscopy; LDH, lactate dehydrogenase; NPs, nanoparticles; PGPB, plant-growth-promoting bacteria; PAA, polyacrylic acid; SEM, scanning electron microscopy; TEM, transmission electron microscopy; XRD, X-ray diffraction; XRPES, X-ray photoelectron spectroscopy.

1. INTRODUCTION

Nanobiotechnology is an emerging field of modern science and technology which has helped us in improving the quality of human life. The synthesis of diverse kinds of nanomaterial (NM) has attracted the interest of the scientists in the last decade due to their wide spectrum applications in the fields of biotechnology, biomedicine, electronics, environmental, food and fuel analysis, and other industries [1-6]. Nanoparticles (NPs) with one or more dimensions of the order of 100 nm or less have demonstrated their merits over their bulk counterparts due to their unique and fascinating properties [7, 8]. Several types of chemical, physical, biological or combination of these methods have been exploited for the synthesis of different kinds of NPs [9-13]. However, physical and chemical methods are commonly employed for the synthesis of NPs but these procedures have some inherent limitations such as chemical methods are highly toxic while the physical ones are very expensive and time consuming [14-16]. Sometimes the use of toxic chemicals in the synthesis of NPs prevents their applications in biomedical fields especially in clinical applications [17, 18] Prabhu. In order to use NPs in clinical fields, there is a need to use reliable, nontoxic and eco-friendly methods for their synthesis. Recently, biological procedures of NPs synthesis have significantly drawn the attention of nanobiotechnologists, although these procedures have some drawbacks. In order to synthesize NPs by an eco-friendly and inexpensive manner, plenty of efforts have been made to replace

currently available conventional chemical and physical methods by biological methods [16].

Biological methods, apart from being inexpensive, also provide protein capped NPs which exhibited very high stability and good dispersity and prevent aggregation of NPs during synthesis [19-21]. These particles may find several applications in a number of disciplines [22-24]. Enzymes are an important group of biomolecules whose catalytic properties can be exploited beyond the limit of conventional chemistry. An enzyme can work under very mild experimental conditions and requires a very low amount of energy. The synthesis of NPs by an enzymatic process has shown its superiority over all known conventional physical and chemical methods. The use of an enzymatic process will eliminate application of costly and toxic chemicals and this procedure is a more acceptable "green" route. It is an eco-friendly and less energy consuming procedure [19, 25].

In this manuscript an effort has been made to describe a brief overview of the recent research activities that focused on the enzymatic synthesis of various kinds of NPs such as metallic, oxide, sulfide and other types of NM. The mechanisms of NPs and NM synthesis and the conditions to control their size, shape and mono-dispersity have been discussed. The characterization of synthesized NPs and other kinds of NM by different techniques have also discussed. The clinical, biomedical and other

applications of NPs synthesized by this procedure have also been summarized in the chapter.

2. OXIDOREDUCTASES

An oxidoreductase catalyzes the transfer of electrons from electron donors, reductants, to the electron acceptors, oxidants. The following reaction is catalyzed by an oxidoreductase.

$$P_i + \text{Glyceraldehyde-3-phosphate} + \text{NAD}^+ \rightarrow \text{NADH} + \text{H}^+ + \text{D-glycerate 1,3-bisphosphate}$$

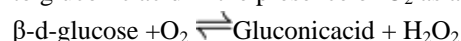
In this reaction, NAD^+ is an oxidant and glyceraldehyde-3-phosphate is a reductant. Oxidoreductases are oxidases and dehydrogenases. Oxidases involve O_2 as an acceptor of hydrogen or electrons whereas dehydrogenases oxidize a substrate by transferring hydrogen to an acceptor that is $\text{NAD}^+/\text{NADP}^+$ or a flavin enzyme. There are some other oxidoreductases i.e., peroxidases, hydroxylases, oxygenases, and reductases. Peroxidases are localized in peroxisomes and catalyze reduction of H_2O_2 . Hydroxylases add hydroxyl groups to its substrates. Oxygenases incorporate oxygen from O_2 into organic substrates. Reductases catalyze reductions, in most of the cases reductases can act as an oxidase [26]. Table 1 summarizes NM obtained by employing oxidoreductases.

Lactobacillus sp. and *Saccharomyces cerevisiae* mediated biosynthesis of TiO_2 NPs has been performed at room temperature. X-ray diffraction (XRD) and transmission electron microscopic (TEM) studies demonstrated formation of TiO_2 NPs. The size of individual NPs as well as few aggregates was 8-35 nm. Concentric Scherrer rings in the selected area of electron diffraction pattern showed NPs of varying orientations. The synthesis of *n*- TiO_2 was catalyzed by pH-sensitive membrane bound oxidoreductases and carbon source dependent rH_2 in the culture solution [27]. In a further study similar group has evaluated the potential of *Saccharomyces cerevisiae* for the synthesis of Sb_2O_3 NPs. The production of Sb_2O_3 NPs has been examined by XRD and TEM and face centered cubic unit cell structure of Sb_2O_3 NPs has been revealed by Rietveld analysis. The shape of the NPs was spherical with 2-10 nm size. The synthesis of *n*- Sb_2O_3 was resulted due to tautomerisation of membrane-bound quinones or the pH-sensitive oxidoreductases. The involvement of endoplasmic reticulum-bound oxygenases in this process has been noticed [28]. Low cost reproducible bacteria, *Aeromonas hydrophila* was employed for the formation of ZnO NPs both as reducing and capping agent. UV-vis spectroscopy, XRD, Fourier transform-infra red (FT-IR), atomic force microscopy (AFM), non-contact atomic force microscopy (NC-AFM) and field emission scanning electron microscopy (FESEM) with energy dispersive X-ray (EDX) were performed in order to confirm the production and characterization of ZnO NPs. The obtained ZnO NPs were characterized by a peak in UV-vis spectrum at 374 nm. AFM exhibited spherical and oval shape of NPs with an average size of 57.72 nm. XRD confirmed the crystalline nature of NPs and Rietveld analysis of the X-ray data indicated that ZnO NPs have hexagonal unit cell at crystalline level. The synthesis of ZnO NPs might be due to variation in the level of rH^2 or pH, which resulted in the activation of pH sensitive

oxidoreductases. The synthesized ZnO NPs were hydrophilic in nature, dispersed uniformly in water, highly stable and exhibited remarkably high antimicrobial activity [29].

More recently Sandana and Rose [30] investigated production of ZnS NPs in quantum regime by *Saccharomyces cerevisiae* MTCC 2918 fungus and characterize their size and spectroscopic properties. Intracellular ZnS NPs were produced by a facile procedure and freeze thaw extraction using 1.0 mM ZnSO_4 . The ZnS NPs showed surface plasmon resonance (SPR) band at 302.57 nm. The produced NPs were in low yield and their obtained size was 30-40 nm. XRD analysis of the powder revealed that the NPs were in the sphalerite phase. Photoluminescence spectra excited at 280 nm and 325 nm exhibited quantum confinement effects. These findings have revealed that yeast cells have sulfate metabolizing systems which is a useful fungal source to assimilate sulfate. Further evidence are needed to understand the transport/reducing processes that result in the synthesis of ZnS NPs such as an oxidoreductase-mediated mechanism.

2.1. Glucose Oxidase. Glucose oxidase (β -d-glucose: O_2 1-oxidoreductase; EC 1.1.3.4) catalyzes the oxidation of β -d-glucose to gluconic acid in the presence of O_2 as an electron acceptor:



Currently microbial glucose oxidases (GODs) have attracted much attention due to their wide spectrum applications in chemical, analytical, pharmaceutical, food, beverage, clinical chemistry, biotechnology and other industries [31-33]. Yasui and Kimizuka [34] explained an enzymatic route for the synthesis of protein-wrapped AuNPs. GOD catalyzed reduction of Au(III) ion in presence of β -D-glucose which resulted in the synthesis of stable AuNPs with diameter of 14.5 nm. FT-IR spectra, zeta potential and circular dichroism (CD) spectra of purified NPs exhibited that the particles were stabilized by adsorbed protein layer. An elegant GOD mediated approach has been adopted for the synthesis of AuNPs of controlled shape and size. In this method GOD was immobilized on solid substrates using layer-by-layer technique. The layer-by-layer films included four alternative layers of chitosan (CS) and poly(styrene sulfonate) by GOD in the uppermost bilayer adsorbed on a fifth CS layer: For the synthesis of AuNPs the films were dipped in the solutions of varying pH containing gold salt and glucose. The highest yield for AuNPs was obtained at pH 9. The size of NPs determined by TEM was 30 nm. Immobilized GOD produced AuNPs more effectively as compared to its free form [35].

2.2. Glutathione Reductase. Glutathione reductase (GR; EC.1.8.1.7) is also known as glutathione-disulfide reductase. It catalyzes reduction of glutathione disulfide (GSSG) to the sulfhydryl form glutathione (GSH). GR works as a dimeric disulfide oxidoreductase and utilizes FAD prosthetic group and NADPH to reduce one mole of GSSG to two moles of GSH [36]. Some workers have evaluated the role of FAD-dependent enzyme, GR in the NADPH-dependent reduction of AuCl_4 and PtCl_6 in

order to synthesize NPs at the active site of the enzyme. The active site of enzyme relatively stabilized very small metallic clusters and prevented their aggregation in absence of a capping ligand. The enzyme synthesized AuNPs at its active site strongly retained via catalytic cysteine. NPs from the active site of the enzyme was released by using β -mercaptoethanol [37, 38]. A novel tellurite reductase from the Antarctic bacterium *Pseudomonas* sp. BNF22 was used to produce tellurium-containing NM. This new enzyme was recognized as GR and was overproduced in *E. coli*. The enzyme was capable of synthesizing Te-containing NM of nearly 68 nm. These NM have exhibited very strong antibacterial activity against *E. coli* and showed no apparent cytotoxic effect against eukaryotic cells [39].

2.3. Glycerol Dehydrogenase. Glycerol dehydrogenase (EC 1.1.1.6) is also called as NAD⁺-linked glycerol dehydrogenase, glycerol: NAD⁺-oxidoreductase. This enzyme belongs to oxidoreductase family that utilizes the NAD⁺ to catalyze the oxidation of glycerol to form dihydroxyacetone [40]. Niide *et al.* [41] have reported an enzymatic synthesis of AuNPs by an engineered *E. coli* harboring a NADH cofactor regeneration system which coupled with glycerol dehydrogenase, its activity was stimulated by adding exogenous glycerol.

2.4. Hydrogenases. Hydrogenases are catalyzing reversible oxidation of H₂ to H⁺ at close to thermodynamic potential. The reaction takes place at a bimetallic active site consisting of Fe atoms ([Fe Fe]-hydrogenases) or one Ni and one Fe atom ([Ni Fe]-hydrogenases), coordinated by biologically unusual CO and CN ligands [42]. Riddin and coworkers [43] reported an enzymatic mechanism for total bioreduction of Pt(IV) into Pt(0) NPs by a mixed consortium of sulphate-reducing bacteria. Two different hydrogenases were involved in this process, firstly the Pt(IV) was reduced to Pt(II) by a two-electron bioreduction using an oxygen-sensitive novel cytoplasmic hydrogenase while in second step Pt(II) ion was reduced to Pt(0) NP by another two-electron bioreduction, involving an oxygen-tolerant/protected periplasmic hydrogenase. The enzyme was identified from its reaction with Cu(II), an active inhibitor of periplasmic hydrogenases. The endogenous electrons were used for the reduction of Pt(II) by the periplasmic hydrogenase in the absence of sulphate. It was noticed that the Pt(IV) ion was completely reduced prior to the reduction of Pt(II) ion. TEM and EDX analysis demonstrated deposition of Pt NPs in the periplasmic space. The incubation of purified dimeric *Fusarium oxysporum* hydrogenase with Pt salt under an atmosphere of hydrogen and optimum enzyme conditions at pH 7.5 and 38°C resulted in the synthesis of Pt NPs. The 90% Pt was reduced in a buffer of pH 9.0 at 65°C in 8 h while 10% of Pt was reduced at pH 7.5 and 38°C within the same time. The bioreduction of Pt salt by a hydrogenase involved a passive process [44, 45].

2.5. Laccase. Laccases (EC 1. 10. 3. 2) are copper-containing oxidases and are present in many plants, fungi, insects and microorganisms. These enzymes catalyze one electron oxidation of various organic and inorganic substrates including mono-, di- and polyphenol aminophenol, methoxyphenol, aromatic amines and ascorbate with the concomitant four electron reduction of O₂

to H₂O [46]. Laccases belong to oxidase family of enzymes and require O₂ as a second substrate for their action. These enzymes catalyze ring cleavage of aromatic compounds [47].

Galliker and coworkers [48] have developed a new system based on laccase-modified silica NPs by examining its potential to degrade a major endocrine disrupting chemical, bisphenol A. The NPs were produced by Stöber method and characterized by SEM, dynamic light scattering (DLS) and z-potential analysis. The introduction of primary amino groups at the surface of the particles was obtained using amino-propyl-triethoxysilane. The use of GA as the bifunctional coupling agent allowed the efficient conjugation of *Corioloropsis polyzona* laccase at the surface of NPs. The oxidative activity of the synthesized bio-conjugate was evaluated by radioactive (¹⁴C) labeled bisphenol A. Sanghi *et al.* [49] have demonstrated the production of AuNPs by fungus *Phanerochaete chrysosporium* after treating with gold ions under ambient aqueous conditions for 90 min. It was found that the laccase was the main enzyme involved in the synthesis of extracellular AuNPs. Ligninase was responsible for the intracellular formation of NPs on the fungal mycelium. The stabilization of NPs via protein layer was confirmed by AFM which showed spherical NPs of 10-100 nm size. These findings demonstrated an important role of fungal enzymes in the synthesis of highly stable AuNPs. Faramaari and Forootanfar [50] used purified laccase from *Paraconiothyrium variable* to synthesize AuNPs. The UV-vis spectrum of gold NPs showed a peak at 530 nm related to SPA of AuNPs represented the formation of AuNPs after 20 min incubation of 0.6 mM HAuCl₄ in presence of 73 U laccase at 70°C. TEM image of AuNPs demonstrated well dispersed NPs in the range of 71-266 nm as determined by the laser light scattering (LLS) method. The pattern of EDX for the prepared gold NPs confirmed its nanocrystal structure. Vetchinkina *et al.* [51] used medicinal basidiomycete *Lentinusedodes* for the reduction of Au(III) from HAuCl₄ to elemental Au [Au(0)], which resulted in the formation of AuNPs. TEM, electron energy loss spectroscopy (EELS), X-ray fluorescence and DLS techniques were employed to characterize NPs. The synthesized NPs have spherical in shape and 5-50 nm size. Laccase, tyrosinase, and Mn-peroxidase were found to be involved in the synthesis of AuNPs.

2.6. Lactate Dehydrogenase. The systematic name for lactate dehydrogenase (LDH; EC 1.1.1.27) is lactate:NAD⁺-oxidoreductase. LDH catalyzes conversion of pyruvate to lactate with concomitant oxidation of NADH during the last step in anaerobic glycolysis [52]. It is present almost in all body tissues. However, when tissues are damaged by injury or disease, they secrete more LDH into bloodstream. Several conditions can cause increased LDH in blood include liver disease, heart attack, anemia, muscle trauma, bone fractures, cancers and infections such as meningitis, encephalitis and HIV. *E. coli* exudate was used for the synthesis of AuNPs at pH 7.35, 30°C and 100 ppm aurochlorate salt. The results were confirmed by UV-vis spectroscopy, XRD and high resolution transmission electron microscopy (HRTEM). HRTEM micrographs as well as SPR peaks of UV-vis spectra showed that obtained AuNPs were of 25-

30 nm size. Further, HRTEM analysis has demonstrated that at inherent pH of reactant spherical NPs were formed while the anisotropic nanostructures were obtained at pH 4. The mechanism of NP formation was decoded using LDH knock out *E. coli*. It was found that LDH knockout bacteria were incapable of synthesizing AuNPs. The role of LDH was further demonstrated when its activity was reduced from $73.5 \mu\text{mol mg}^{-1} \text{min}^{-1}$ to $24 \mu\text{mol mg}^{-1} \text{min}^{-1}$ in normal *E. coli* [53].

2.7. NADH-Dependent Reductase. NADH is employed as a most common reduced coenzyme in redox reaction in an organism and thus it is participating as a reducing agent *in vivo* in many enzymes catalyzed reactions [54, 55]. It has been noticed that *A. terreus* NADH-dependent reductase involved in the synthesis of AgNPs. The silver ions received electrons from NADH via NADH-dependent reductase and then reduced to Ag. Several earlier workers have also reported the involvement of NADH-dependent reductases from *Fusarium oxysporum* and *P. fellutanum* during biosynthesis of AgNPs [44, 56]. Li et al. [57] have reported reduction of aqueous Ag^+ ion by the culture supernatants of *Aspergillus terreus* for the purpose of synthesis of AgNPs. The reaction occurred at ambient temperature and in a very short time. The bioreduction of AgNPs was monitored by UV-vis spectroscopy. The obtained AgNPs were polydispersed spherical as characterized by TEM and XRD. The size of NPs was in a range of 1-20 nm. The obtained NPs were quite stable and were produced without the participation of any toxic chemicals as capping agents. Reduced NADH was found to be an important reducing agent during the formation of AgNPs in an enzyme-mediated extracellular reaction process. NADH and NADH-dependent reductase were found key players in the synthesis of AgNPs. The as-synthesized NPs have efficiently inhibited various pathogenic organisms, including bacteria and fungi. Correa-Llantén et al. [58] have described the generation of AuNPs by thermophilic bacterium *Geobacillus* sp. strain ID17. Cells exposed to Au^{3+} turned from colorless into an intense purple color. The elemental analysis and composition of NPs were determined by TEM and EDX investigation. The intracellular localization and particles size of NPs was confirmed by TEM which illustrated two different types of particles of predominant quasi-hexagonal shape with 5-50 nm size. The majority of the particles were in a range of 10-20 nm. FT-IR spectroscopy was used to characterize chemical surface of AuNPs. In an earlier study the involvement of reductase activity in the synthesis of AuNPs by some other microorganism has also been reported, where the reduction was initiated by the electron transfer from NADH via a NADH-dependent reductase and thus it involved in the reduction of Au^{3+} [59]. This reduction using NADH as substrate was evaluated in ID17 and it was found that the crude extracts of the microorganism catalyze NADH-dependent biosynthesis of AuNPs by ID17.

2.8. Nitrate Reductase. Nitrate reductase is a multi-domain enzyme which is made up of prosthetic groups molybdopterin, Fe-heme, and FAD in a 1:1:1 stoichiometry that mediates an electron transfer from NADPH to nitrate. The FAD and Mo-pterin domains function as the binding sites for NADPH and NO_3^- , respectively. However the cytochrome b_5 -like heme domain facilitates electron

transfer from FAD domain to the active-site Mo-pterin [60]. In an earlier study, Durán and coworkers [61] have described the reduction of aqueous silver ions into silver hydrosol by the exposure of several *Fusarium oxysporum* strains. The size of obtained AgNPs was in the range of 20-50 nm. This reduction of metal ions was mediated by a nitrate-dependent reductase and a shuttle quinone extracellular process. The produced NM expressed very high antibacterial activity. *In vitro* synthesis of AgNPs by α -NADPH dependent nitrate reductase and phytochelatin have been demonstrated. The silver ions were reduced in presence of nitrate reductase and thus it produced stable silver hydrosol of 10-25 nm diameters. These NPs were stabilized by capping peptide. XRD, TEM, XRPES and UV-vis absorption techniques were used for the characterization of NPs [62]. The filtrate from fungus *Fusarium semitectum* has been used for the extracellular synthesis of highly stable and crystalline AgNPs from silver nitrate solution. The production of NPs was evaluated by UV-vis spectroscopy and XRD analysis. Majority of synthesized NPs were spherical in shape as visualized by TEM and their obtained size was 10-60 nm. The reduction of Ag^+ to Ag^0 was mediated by an enzyme present in organism. It was recorded that the exposure of Ag ions to *F. oxysporum* caused release of nitrate reductase and subsequent formation of remarkably stable AgNPs. These NPs showed antibacterial activity [63, 64].

In a further investigation, Vaidyanathan and coworkers [65] reported the synthesis of AgNPs by nitrate reductase. The obtained NPs were characterized TEM and the size of NPs was in the range of 10-80 nm. These NPs were employed in various medical applications. Marine macro alga *Sargassum wightii* was used for synthesis of AuNPs. A remarkable reduction in the nitrate reductase activity was noticed after fabrication of AuNPs. The morphology of the fabricated AuNPs was visualized by electron microscopy which showed the presence of isotropic spheres along with anisotropic NPs. The size of the obtained NPs was from 30-100 nm. XRD was used to evaluate the crystalline nature of AuNPs and it was found to be face centered cubic [66]. The leaf extract of *Adathoda vasica* a tropical shrub was considered in order to convert gold ions into monodispersed AuNPs. The maximum production of NPs was obtained at 80-100°C, pH 6 and 50 ppm of aurochlorate. These NPs were characterized by UV-vis spectroscopy, XRD and HRTEM. The obtained size of AuNPs was 10-20 nm. It was observed that nitrate reductase and glutathione were the main reducing agents in the synthesis of AuNPs [67]. In further study these workers demonstrated a green nanotechnological procedure for the biosynthesis of AuNPs by exploiting the reducing and thermodynamically efficient molecular mechanisms of medicinal plant, *Asparagus racemosus*. FT-IR analysis has shown the role of glutathione as one of the capping agent and biochemical assays exhibited the involvement of nitrate reductases as reducing agent during synthesis of AuNPs. The nitrate reductase and capping protein activities were reduced after biofabrication of AuNPs. The electron microscopy and XRD were employed to examine morphology and crystal structure of AuNPs, respectively [68].

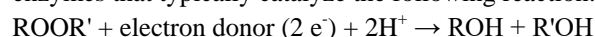
El-Batal and colleagues [69] have employed culture supernatant of *Bacillus stearothermophilus* for synthesis of AgNPs by reduction of silver ions via nitrate reductase. Synthesized AgNPs were characterized by TEM, DLS, FT-IR and UV-vis spectroscopic analysis. The antimicrobial activity of the NPs was monitored against some pathogenic multidrug-resistant strains of yeast, Gram-negative and Gram-positive bacteria by using Kirby-Bauer method. The inhibition of microbial growth of the investigated strains was in the order of *Candida spp*>Gram-positive bacteria>Gram-negative bacteria. The synthesis of AgNPs by a probiotic microbe has been examined. The synthesized NPs was investigated by UV-vis spectroscopy and characterized by UV spectra, FT-IR analysis, SEM with energy dispersive spectroscopy (EDS) and using particle size analysis. Nitrate reductase assay showed its involvement in the synthesis of NPs. The bactericidal effect against common Gram-positive and Gram-negative bacteria has also been demonstrated. The results exhibited high antimicrobial activity against Gram-negative organism [70]. Mewada et al. [71] described formation of AuNPs by *Pseudomonas denitrificans* exudates and they noticed participation of nitrate reductase in the reduction of gold. UV-vis spectroscopy and HRTEM were employed for analysis of optical properties and morphology of NPs and the measured size of NPs was from 25-30 nm. XRD was used to determine crystalline nature of AuNPs and it was found to be face centered cubic. FT-IR analyses of NPs having sulphhydryl, amido, carbonyl functional groups which demonstrated role of peptides in capping the NPs in order to provide them stability. *Penicillium sp.* was used for the extracellular synthesis of AgNPs and this process of reduction of silver ions into AgNPs was due to involvement of nitrate reductase. The formation of AgNPs was monitored by UV-vis spectrophotometry. The size of AgNPs was 75 nm as determined by AFM [72].

Gunasekar and coworkers [73] have constructed three TiO₂ samples i.e., TiO₂ (TiO₂-A), biotemplated TiO₂ (TiO₂-B), and enzyme, nitrate reductase mediated Ag-TiO₂ biotemplate (TiO₂-C). XRD, FESEM, EDS and UV-vis-NIR spectroscopy were used to examine the presence of anatase phase of TiO₂ and silver in synthesized complex. Photocatalytic efficiencies of these photocatalysts were evaluated for oxidation of reactive black dye under solar light irradiation in batch reactors. Photocatalytic efficiencies of samples were compared by statistical tools like one-way ANOVA and Tukey test. The findings of this work have shown that photocatalytic efficiency of TiO₂-C was 40% higher than that of TiO₂-A under solar light irradiation. Fernando et al. [74] have screened 12 plant-growth-promoting bacteria (PGPB) and 4 actinomycetes isolate from Philippine soils and investigated their roles in the synthesis of gold NPs from ionic gold. They observed the participation of nitrate reductase in the bioreduction of ionic gold. Only 10 PGPBs exhibited nitrate reductase activity after 5 d of incubation at 37°C. PGPB culture supernatants were incubated with gold (III) chloride trihydrate for 7 d at 28°C for *in vitro* synthesis of AuNPs. UV-vis scanning spectroscopy of the culture supernatants of PGPBs 1 and 5 showed absorbance peaks of AuNPs at 570 nm and 541 nm, respectively. TEM analysis of

PGPBs 1 and 5 exhibited the presence of AuNPs of 10-100 nm size. SEM and EDX analysis showed the formation of AuNPs by PGPB 5.

Recently it has been noticed that chromosomally encoded silver resistance determinant of *E. coli* strain produced AgNPs in periplasmic space when it was exposed to Ag(I) salts. The synthesized AgNPs were present in zero-valent metallic silver lattice form. The production of such NPs was favorable under anaerobic conditions; it showed biological reduction of Ag⁺ ions. The role of microbial c-type cytochromes has been evaluated in the formation of AgNPs. A deletion mutant of the cytoplasmic membrane-anchored tetra-heme c-type cytochrome subunit of periplasmic nitrate reductase (NapC) exhibited a marked decrease in the synthesis of AgNPs. Moreover, the re-introduction of NapC has further retained biosynthetic property of AgNPs. Thus this investigation has confirmed the participation of c-type cytochrome during synthesis of AgNPs [75]. The production of AgNPs was obtained by using a purified fungal nitrate reductase in presence of gelatin as a capping agent and these NPs exhibited very strong biological activity against human pathogenic fungi and bacteria. NPs were characterized by XRD, DLS spectroscopy, SEM and TEM. The stable non-aggregating NPs were spherical in shape with an average size of 50 nm and a zeta potential of -34.3 [76].

2.9. Peroxidase. Peroxidases (EC 1.11.1.x) are a large family of enzymes that typically catalyze the following reaction:



Most of these enzymes require optimal substrate as H₂O₂, but some of them are active in the presence of organic hydroperoxides such as lipid peroxides [77, 78]. The chiral conducting PANI NC [polyacrylic acid (PAA)/PANI(-) camphorsulphonic acid (CSA)] were synthesized by HRP in a buffer, pH 4.3. It was noticed that HRP played an important role in the polymerization, which allowed PANI to prefer a specific helical conformation whether the induced chirality in the monomer-CSA complex is either by (+)CSA or (-)CSA. The structural characterization of NC was made by solid state ¹³C cross-polarization with magic angle spinning NMR techniques. The structural features of PANI in the conducting form of synthesized NC were similar to chemically synthesized PANI [79]. Three methods were developed for the synthesis of DNA-templated PANI nanowires and networks. Oxidative polymerization of PANI in the buffer of moderate pH was completed using ammonium persulfate as an oxidant or alternatively HRP mediated oxidation, or by ruthenium complex mediated photo-oxidation. It has been observed by AFM that all three methods led to the preferential growth of PANI along with DNA templates. PANI was immobilized on the surface of DNA templates. Current-voltage measurements were done on DNA/PANI networks synthesized by either enzymatic method or by photo-oxidation. The conductance was consistent with values measured for undoped PANI films [80].

A biocatalytic procedure was followed for the production of conducting PANI-NPs. This procedure involved in the synthesis of NC of PANI and PAA by polymerizing aniline-CSA macromonomer using HRP in presence of template PAA. The second step included the separation of PANI polymers from PAA

and CSA in NC. TEM analysis was used to investigate the creation of PANI-NPs by the two-step approach. High-resolution solution ^{13}C NMR and UV-vis spectroscopic techniques were employed to monitor the formation of conducting PANI chains by this method [81]. HRP catalyzed oxidative polymerization of aniline to form conductive PANI. This process was enhanced by the presence of a macromolecular template with sulfonic acid groups which developed a unique environment for the formation of conducting polymer. These investigators have used a photo-cross-linkable thymine-based polymer with phenylsulfonate groups as a template substrate for this synthesis [82]. PANI colloidal particles were produced by HRP catalyzed polymerization of aniline employing CS as steric stabilizer and toluene sulfonic acid (TSA) or CSA as doping agents. FT-IR and UV-vis spectroscopic analysis exhibited that enzymatic polymer formation of aniline in dispersed media which produced emeraldine salt form of PANI. TEM was used to examine the morphology of colloids. CSA produced rod-like particles while TSA formed mainly oblong particles. PANI particles with high colloidal stability and size below 200 nm were achieved in the presence of 1.0 wt% of CS in reaction media, showing that this polymer was highly effective as a steric stabilizer. About 20 wt% CS was attached to the PANI. The colloids obtained either by TSA or CSA demonstrated a strong pH-dependent colloidal stability and underwent rapid flocculation in near neutral or alkaline media. This fascinating property of the colloids might be employed in separation technology [83]. Nabid *et al.* [84] reported an enzymatic method for synthesis of conducting NC between PANI and anatase TiO_2 NPs. The presence of sulfonated polystyrene (SPS) affects the polymerization reaction and this reaction is catalyzed by HRP. For forming a core-shell structure PANI was deposited on the surface of TiO_2 . The synthesized NC was characterized by FT-IR, UV-vis spectroscopy and SEM analysis. These findings showed a strong binding at the interface of PANI and nano- TiO_2 . The ability of PANI and PANI/ TiO_2 NPs for electron exchange by Pt electrode, by casting the PANI and PANI/ TiO_2 NPs on the Pt electrode surface was examined by cyclic voltammetry. Difference of anodic and cathodic peak potential and formal potential values for PANI (281 mV and 425.5 mV, respectively) and PANI/ TiO_2 NPs (39 mV and 591.5 mV, respectively) were analyzed by voltammograms. Gao *et al.* [85] evaluated the self-assembly and transformation of nanostructures controlled by enzymatic kinetics in a system consisting of HRP, H_2O_2 and 3,3',5,5'-tetramethylbenzidine (TMB). Numerous TMB derivatives were obtained in the system in presence of varying concentrations of HRP which assemble into nanoscale structures in a number of morphologies and colors. These assemblies were reversible under physiological conditions. The synthesis and controlling of such "nano-transformers" via enzymatic kinetics will expand new areas for the formation of smart materials and biomimetic nanofabrication. Ryu *et al.* [86] have prepared for the

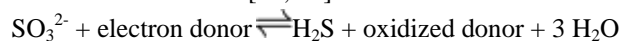
first time composites of MWCNT and polypyrrole (Ppy) by HRP catalysis. Electron micrographs showed that the *in situ* enzymatic reaction by HRP resulted in uniform coating of MWCNT with Ppy without containing the polymer aggregates. The specific capacitance of the composites (46.2 F g^{-1}) measured with a two-electrode cell containing an electrolyte of $1 \text{ mol L}^{-1} \text{ NaNO}_3$ increased more than 4-fold compared with that obtained with bare MWCNT (10.8 F g^{-1}). *In situ* enzymatic polymerization of aniline onto MWCNT and COOH-MWCNT was evaluated in order to produce NC. HRP was used to catalyze polymerization of aniline in the presence of H_2O_2 at room temperature in a buffer of pH 4. FT-IR, SEM, TEM and thermo-gravimetric analysis (TGA) were used for the characterization of NC. TEM analysis exhibited tubular morphology with uniformly distributed MWCNT in the NC. SEM and TEM exhibited wrapping of the MWCNT with PANI chains. TGA demonstrated that the PANI component was thermally more stable in PANI/COOH-MWCNT than PANI/MWCNT composites. The synthesized NC had higher conductivity than pure PANI and it was due to a strong interaction between PANI chains and MWCNT [87]. GO/PANI NC was produced by HRP catalyzed polymerization of aniline in aqueous acidic medium using TSA as doping agent and H_2O_2 as an oxidizer. Two GO dispersions with sheets of an average lateral size of $12.50 \mu\text{m}$ and 247 nm were taken. The polymerization reaction was examined using 1.0, 2.5 and 5 wt % of GO and nGO dispersions. The attachment of PANI colloids with GO sheets was monitored by SEM. The characterization of PANI-GO colloids was done by FT-IR and UV-vis spectroscopy. The colloidal stability of NC was determined in the buffer of different pH [88]. The AgNPs were synthesized by peroxidase reduction and silver enhancement kit, EnzMetTM from Nanoprobes. The structures of AgNPs films of different densities were examined by SEM and TEM. TEM evaluated cross sections of AgNPs, were further investigated in order to confirm their chemical composition by EDX spectroscopy. The surface coverage of substrates by AgNPs and the maximum particles height was determined by Rutherford backscattering spectroscopy. The initial growth state the AgNPs exhibit desert-rose or nano-flower structure. It is indicated the desert-rose-like AgNPs consist of single-crystalline plates of pure silver [25]. Tetronic-grafted CS containing tyramine moieties was used for HRP-mediated hydrogel formation *in situ*. This gel was useful for loading NPs of biphasic calcium phosphate, mixture of hydroxyapatite and tricalcium phosphate, forming injectable biocomposites. HRP catalyzed the production of hydrogel composites in the suspension of copolymer and biphasic Calcium phosphate NPs. The compressive stress failure of the wet hydrogel was at $591 \pm 20 \text{ KPa}$ with the composite 10 wt% biphasic calcium phosphate loading. The composite was biocompatible and cells were well-attached on the surfaces. The experiment was performed *in vitro* by using mesenchymal stem cells [89].

Table 1. Biosynthesis of NM by Using Oxidoreductases.

Name of enzyme	Name of NPs	Size (nm)	Shape	Reference/s
Oxidoreductases	ZnO	57.72	Spherical & oval	[29]

Name of enzyme	Name of NPs	Size (nm)	Shape	Reference/s
Oxidoreductases	ZnS	30-40	Sphalerite	[30]
Glucose oxidase	Au	14.5	----	[34]
Glucose oxidase	Au	30	----	[35]
GR, Thioredoxin reductase, lipoamide dehydrogenase	AuCl ₄ & PtCl ₆ ²⁻	-----	-----	[37, 38]
Ligninase	Au	10-100	Spherical	[49]
Laccase	Au	71-266	Nanocrystal	[50]
Laccase/Tyrosinase	Au	5-50	Spherical	[51]
/Mn peroxidase				[53]
Lactate dehydrogenase	Au	25-30	Spherical	
Sulfate reductase	CdS	---	Q-state	[92]
NADH dependent reductase	Ag	1-20	Spherical	[57]
NADH dependent Reductase	Au	5-50	Quasi-hexagonal	[58]
NADH dependent nitrate reductase	Ag	20-50	Hydrosol	[61]
Nitrate reductase	Ag	10-25	Hydrosol	[62] [63, 64]]
Nitrate reductase	Ag	10-60	Spherical	
Nitrate reductase	Ag	10-80		[65]
Nitrate reductase	Au	30-100	Isotropic spheres	[66]
Nitrate reductase	Au	10-20	Monodispersed	[67]
Nitrate reductase	Au		Crystal	[68]
Nitrate reductase	Ag	50	Spherical	[76]
Sulphite reductase	CdS	5-20	Quantum dots	[93] [94]
	Au	7-20	Gold hydrosol	
Sulphite reductase	Co ₃ S ₄ , PbS, Ni ₇ S ₆	---	Quantum dots	[95]

2.10. Sulphite/Sulfate Reductase. Sulfite reductases (EC 1.8.99.1) belong to the family of oxidoreductases and are present in archaea, bacteria, fungi and plants. These enzymes catalyze reduction of sulfite to H₂S and H₂O. The reaction obtained electrons from the dissociable molecules of either NADPH, bound flavins or ferredoxins [90, 91].



Ahmad *et al.* [92] have demonstrated production of Q-state CdS NPs by reaction of aqueous CdSO₄ solution with fungus, *Fusarium oxysporum*. The formation of NPs started by release of sulfate reductase from the fungus and this enzyme catalyzed the conversion of sulfate ions into sulfide ions that subsequently react with aqueous Cd²⁺ ions to yield highly stable CdSNPs. The *in vitro* synthesis of CdS quantum dot NPs have been achieved by using sulphite reductase and capping peptide in the presence of a co-factor NADPH. Sulphite reductase catalyzed production of CdSNPs of 5-20 nm dimensions in aqueous solution of CdCl₂, Na₂SO₃ and capping peptide in the presence of NADPH. These CdSNPs were coupled to plant lectins, jacalin and chick pea lectin by 1-ethyl-3-(3-dimethylaminopropyl) carbodiimide mediated coupling. These eco-friendly synthesized CdSNPs have shown their application as fluorescent biolabels [93]. α -NADPH-dependent sulfite reductase and phytochelatin were used for *in vitro* synthesis of AuNPs. The gold ions were reduced in presence of sulfite reductase which led to the formation of a stable gold hydrosol of 7-20 nm size. These NPs were stabilized by capping peptide and were characterized by XRD, TEM, X-ray

photoelectron spectroscopy (XRPES) and UV-vis optical absorption [94]. Further, Ansary and colleagues [95] have demonstrated the use of sulfite reductase along with synthetic peptides for *in vitro* formation of control particle size metal sulfide quantum dots viz. Co₃S₄, PbS and Ni₇S₆. Sulfite reductase was incubated with aqueous solution of CdCl₂, or Co(NO₃)₃ or NiCl₂ or Pb(NO₃)₂, and Na₂SO₃ in presence of a suitable capping peptide that produced controlled particle size CdS, Co₃S₄, Ni₇S₆, or PbS quantum dots, respectively. Absorbance and photoluminescence spectrometry, XRD, XRPES and HRTEM techniques were used for the characterization of sulfite reductase synthesized and size controlled metal sulfide quantum dots. A temperature and sodium dodecyl sulphate resistant sulfite reductase was purified from extremophilic actinomycete *Thermomonospora* and was employed for the synthesis of AuNPs along with the capping molecule, which produced AuNPs monodispersed in solution [96]. Gholami-Shabani *et al.* [97] used α -NADPH-dependent sulfite reductase purified from *Escherichia coli* for cell-free synthesis of gold NPs. The obtained NPs were spherical with an average size of 10 nm and a zeta potential of -30 ± 0.2 and demonstrated remarkably high antifungal activity towards a wide range of human pathogenic fungi. These NPs exhibited no toxicity for two cell lines, *i.e.*, Vero and Hep-2 at the concentrations ranging from 0.31 to 10%. In a most recent study these workers have further developed a cell-free system for the biosynthesis of AuNPs using a fungal sulfite oxidoreductase from *Fusarium oxysporum*. The obtained NPs were spherical in shape with an average size of

20 nm as determined by SEM, TEM and DLS. NPs showed very high growth inhibitory activity against all tested human

pathogenic yeasts and molds [98].

3. HYDROLASES

3.1. Carbohydrases.

Table 2 lists NM synthesized by the involvement of carbohydrases.

3.1.1. α -Amylase . α -Amylase (EC 3.2.1.1) hydrolyses α bonds of large, α -linked polysaccharides, such as starch, glycogen and other related polysaccharides yielding glucose and maltose. The official names of enzymes is 1,4- α -D-glucan glucanohydrolase; which is maintained by a commission on enzyme nomenclature. It is the major form of amylase found in humans and other mammals [99]. It is also present in seeds containing starch as a food reserve and is secreted by many fungi. Rangnekar *et al.* [100] used α -amylase to synthesize and stabilize AuNPs in aqueous solution. The activity of enzyme was retained in AuNP- α -amylase complex. The presence of AuNPs and α -amylase in complex was confirmed by UV-visible and FT-IR spectroscopy, XRD and TEM measurements. It was noticed that the presence of free and exposed SH groups was essential during reduction of AuClO₄ to AuNPs. The structural analysis of α -amylase showed the presence of free and exposed SH groups in its native state and thus the enzyme was found suitable for the production of NPs. Some investigators have evaluated synthesis of AuNPs by an extracellular α -amylase for the reduction of AuCl₄ with the retention of enzymatic activity in the complex. The enhanced synthesis of particles was achieved by optimizing the medium components for α -amylase. The NPs size was determined by TEM analysis as 10-50 nm [101]. The α -amylase was employed to synthesize NPs of five metal ions; i.e., Cu⁺², Se⁺⁴, Bi⁺⁴, Au⁺³, Ag⁺¹, among which Au, Ag and Au/Ag alloy NPs were successfully synthesized and characterized. Maximum absorbance at 530, 440 and 458 nm related to the formation of AuNPs, AgNPs and Au/AgNPs, respectively, were determined by UV-vis spectroscopy. The biosynthesis of nanostructures by α -amylase was probed by SEM equipped with EDX microanalyser. Two intense peaks at 1620 cm⁻¹ and 3430 cm⁻¹ in FT-IR spectra of obtained NPs were related to carbonyl and OH/NH groups, respectively. The size of AuNPs, AgNPs and Au/Ag alloy NPs, analyzed by LLS method, was determined to be 89 nm, 37 nm and 63 nm, respectively [102]. Further, biosynthesis of Au, Ag and Au-Ag alloy NPs was mediated by α -amylase at 70°C in 0.1 mM AgNO₃. The average particles sizes determined by LLS method for Au, Ag and Au/Ag alloy NPs were 86 nm, 37 nm and 63 nm, respectively [103]. Mishra and Sardar [104] have used α -amylase for the synthesis of AgNPs. The silver ions were reduced to stable AgNPs by α -amylase. The synthesized NPs were characterized by UV-visible absorption and TEM analysis. TEM study demonstrates mono-disperse NPs of 22-44 nm diameters with 22-44 triangular and hexagonal shape. UV-vis measurement exhibited absorption band at 422 nm due to SPR. Arunkumar *et al.* [105] exploited bioreductive potential of *Micrococcus luteus* for eco-friendly synthesis of AuNPs. Biochemical and physiological analysis showed that AuNPs production was due to dual mode

which involved extracellular α -amylase and cell wall teichuronic acid of *Micrococcus luteus*. Isolated bacterial α -amylase and teichuronic acid reduces Au³⁺ into Au which resulted in the synthesis of AuNPs. These NPs were stable for more than one month. The characterization of synthesized AuNPs was done by UV-vis spectrophotometry, TEM, FT-IR and DLS analysis. The obtained AuNPs were found to be mono-dispersive and spherical in shape with an average size of 6 nm and 50 nm for α -amylase and teichuronic acid, respectively. In a further study, Mishra and Sardar [106] have used α -amylase as a sole reducing and capping agent for the production of AuNPs. The formation of AuNPs in 6 h was confirmed SPR band at 525 nm. The obtained gold NPs were characterized by TEM, HRTEM, DLS and XRD. The synthesized NPs catalyzed degradation of *p*-nitroaniline and *p*-nitrophenol in aqueous solutions. Most recently the same group has produced TiO₂ NPs by using α -amylase as a reducing and capping agent. XRD and TEM analysis were employed for characterization of obtained NPs. The monophasic crystalline nature of NPs was confirmed by XRD. The antibacterial effect of these NPs was monitored on *S. aureus* and *E. coli* and MIC of TiO₂ NPs was observed as 62.50 g mL⁻¹ for both bacterial strains [107].

3.1.2. Dextranase. Dextranase (EC 3.2.1.11, dextran hydrolase) is an enzyme with systematic name as 6- α -D-glucan-6-glucanohydrolase. It catalyzes endohydrolysis of (1-6)- α -D-glucosidic linkages in dextran. Kim and Walsh [108] have successfully synthesized CuS, Cu_xS, Ag₂S and CdS NPs using a novel green procedure to give dextran biopolymer stabilized metal sulfide nanosuspensions. In this reaction dextranase was used to remove bulk of the bound dextran in order to get pure stable metal sulfide nanocrystals for their applications in medicine, photonics and solar cells. Particles of good homogeneity were obtained. The size of NPs for CuS, Cu₂S, Ag₂S and CdS was 9-27 nm, 14 nm, 20-50 nm and 9 nm, respectively. NPs were characterized by TEM, XRD, TGA, FT-IR and zeta-potential measurement and their UV-vis spectroscopic absorption properties were determined. This procedure has demonstrated very high potential for the large scale production of a range of functional sulfide NPs.

3.1.3. β Galactosidase. β Galactosidase was used to synthesize AgNPs and UV-vis spectroscopy was used to screen SPR peaks of AgNPs. The size of NPs was 12.89 \pm 0.16 nm as visualized by TEM and the obtained NPs were fine spherical and quasi-spherical shape as examined by SEM. The crystallinity and presence of elemental silver were revealed by XRD and EDS. The antimicrobial potential of AgNPs was evaluated against pathogenic bacterial strains of *E. coli*, *S. aureus*, *P. aeruginosa* and *S. epidermidis*. The obtained AgNPs showed very high bactericidal and dye decolorization activity. The as-prepared AgNPs did not show any cytotoxic effect as examined on peripheral blood lymphocytes *in vitro*. The findings of the work demonstrated that environmentally friendly method was quite efficient in the synthesis of AgNPs [109].

3.1.4. Endoglucanase. β -1,4-endoglucanase (EC: 3.2.1.4) is an enzyme that catalyzes the endohydrolysis of cellulose, lichen and cereal β glucans. It is produced mainly by fungi, bacteria, and protozoans. Recently nanocellulose from cellulosic biomass has attracted the attention of nanobiotechnologists due to their biodegradable nature, low density, high mechanical properties, economic value and easy availability [110]. The enzymatic synthesis and functionalization of nanocellulose from lignocelluloses have already been reviewed [111]. Henriksson *et al.* [112] have treated cellulosic wood fiber pulps by endoglucanases or acid hydrolysis in combination with mechanical shearing in order to disintegrate MFC from the wood fiber cell wall. The produced MFC nanofibers were studied by AFM. It is noticed that the enzymatic-treatment of cellulosic wood fiber pulp facilitate disintegration and MFC nano-fibers production. Cellulose nanocrystals (CNC) from recycled pulp were prepared by an endoglucanase. The maximum amount of CNC was produced by treatment with 84 U of endoglucanase per 200 mg recycled pulp at 50°C for 60 min of microwave and conventional heating. Two types of heating were involved in this synthesis. Microwave heating at each treatment gave a greater amount of product as compared to conventional heating. TEM and SEM analysis of suspensions demonstrated CNC with widths of 30-80 nm and lengths of 100 nm-1.8 μ m. It was within the limit of the length of CNC, 100 nm-3.5 μ m, obtained by DLS analysis. The average zeta potential of CNC was -31.37 mV. XRD of CNC, recycled pulp and residues of recycled pulp exhibited a gradual change in the particle size [113]. Bacterial CNC were obtained by using commercially available cellulase. AFM and TEM were employed for the evaluation of morphology and dimensional parameters of the CNC. The thermal stability and activation energy of enzymatically produced CNC was much higher as compared to sulfuric acid processed ones [114].

Cellulase from *Trichoderma reesei* was used to synthesize CNC by controlled hydrolysis of bamboo fibers. FESEM and XRD were used to characterize morphology and crystallinity of CNC fibers, respectively. The degree of polymerization was examined by automatic viscosimeter. The surface charge in suspension was measured by zeta-potential. All CNC fibers were found in a rod-like shape with an average diameter of 24.7 nm and length of 286 nm, with an aspect ratio of around 12. The zeta potential of cellulase hydrolyzed CNC was 4-times less than that produced by acid hydrolysis [115]. *Aspergillus niger* cellulase was exploited for the production of CNC and microcrystalline cellulose from solubilized kraft pulp feedstock with minimal processing and that a chimeric cellulase partially digested kraft pulp and live wood feedstock [116].

3.2. Proteolytic Enzymes.

Table 3 represents NPs synthesized by proteolytic enzymes.

3.2.1. Bacterial protease. Bharde *et al.* [117] evaluated the formation of anisotropic AuNPs biologically by using bacterium *Actinobacter* spp. They challenged bacterium with gold chloride in the presence of bovine serum albumin (BSA). The generation of AuNPs was taking place by simultaneous induction of a protease secreted by the bacterium in presence of BSA. The presence of BSA helps to enhance the rate of AuNPs biosynthesis and may also participate in controlling shape.

3.2.2. R-chymotrypsin. Chymotrypsin (CHT, EC 3.4.21.1) is a digestive enzyme. It is a component of pancreatic juice and it catalyzes proteolysis of proteins and peptides in duodenum. CHT preferentially hydrolyzes peptide/amide bonds where the carboxyl side of the amide bond (P_1 position) has a large hydrophobic amino acid i.e., tyrosine, tryptophan and phenylalanine. It also cleaves other types of amide bonds in peptides at slower rates particularly those containing leucine and methionine at the P_1 position [118]. Narayanan *et al.* [119] have discussed the synthesis of CdSNPs directly conjugated to CHT by chemical reduction in aqueous solution. Matrix-assisted laser desorption ionization mass spectrometry exhibited strong conjugation of CdSNPs to CHT via covalent bonding in CdS-CHT conjugates. HRTEM analysis showed that CdSNPs are well dispersed with an average diameter of 3 nm, and EDX elemental analysis demonstrated composition of CdS-protein conjugates. The CD analysis was used to examine the structural integrity of CHT before and after binding to CdSNPs. The functional integrity of CHT after conjugation with CdSNPs was investigated by monitoring the enzymatic activities of CHT and CdSNPs bound CHT by absorption spectroscopy.

3.2.3. Curcain. Curcain is a proteolytic enzyme and it is obtained from *Jatropha curcas* shoots. It shows wound healing property in mice [120]. Hudlikar *et al.* [121] synthesized ZnSNPs by using 0.3% *Jatropha curcas* L latex solution. ZnSNPs were characterized by XRD, selected area electron diffraction, TEM, EDX, UV-vis optical absorption and photoluminescence techniques. FT-IR spectroscopy was performed to find out the role of cyclic peptides namely curcacycline A, curcacycline B and curcain which acts as a reducing and stabilizing agents present in the latex of *J. curcas* L. The average size of ZnSNPs was found to be 10 nm. Latex of *J. curcas* L. was also the source for sulphide (S^{2-}) ions that are donated to Zn ions under present experimental conditions. Source of sulphide (S^{2-}) ions is still unknown, but it is expected that cysteine or thiol residues present in enzyme curcain may be donating sulphide (S^{2-}) ions. Further these workers have prepared TiO_2 NPs by using 0.3% aqueous extract from latex of *Jatropha curcas* L. The NPs were characterized by XRD, selected area electron diffraction, TEM, EDX and FT-IR. FT-IR was formed in order to understand the role of curcain, curcacycline A and curcacycline B as possible reducing and capping agents, present in the latex of *J. curcas* L. The mean size of NPs was from 25-100 nm. These findings have indicated the presence of two broad categories of NPs. First types of NPs were spherical in shape with diameter from 25-50 nm while the second types were larger and uneven shapes NPs [122].

3.2.4. Papain. Papain (EC. 3.4.22.2) is a thiol protease. It is present in the leaves, latex, roots, and fruit of the papaya plant (*Carica papaya*) that catalyzes the breakdown of proteins. Papain is used in biochemical research involving the analysis of proteins, in tenderization of meat, clarifying beer, removing hair from hides before tanning and as a cleansing agent for soft contact lenses. It is also used in toothpastes and cosmetics and in preparations of various remedies for indigestion, ulcers, fever and swelling [123, 124]. Gold nanoclusters have been for the first time synthesized by using papain as a capping and reducing agent. Various optimal conditions such as concentrations of papain and NaOH, reaction time and temperature for the synthesis of gold nanoclusters have

been standardized. The synthesized gold nanoclusters exhibited intense red emission at 660 nm (QY 4.3%) and are uniform in size. The clusters are quite stable and the intense red emission remained unchanged in the range of buffers, pH 6-12. The fluorescent gold nanoclusters were employed as a label-free probe for the sensitive detection of Cu^{2+} upto 3 nM [125].

3.2.5. Serratiopeptidase. Serratiopeptidase (EC 3.4.24.40) is a proteolytic enzyme obtained from *Serratia* sp. E-15. This microorganism was originally isolated in late 1960s from silkworm *Bombyx mori* L., intestine. It dissolves its cocoon. This enzyme is prescribed in several specialties like surgery, orthopaedics, otorhinolaryngology, gynaecology and dentistry for its anti-inflammatory, anti-edemic and analgesic effects. Some anecdotal reports have described anti-atherosclerotic effects due to its fibrinolytic and caseinolytic properties [126]. Venkatpurwar & Pokharkar [127] studied synthesis of AuNPs by using a therapeutic enzyme serratiopeptidase at 25°C and in buffer, pH 7.0. UV-vis spectroscopy, TEM, XRD and FT-IR spectroscopy were used for identification and characterization of AuNPs. Proteolytic enzyme assay showed that the composite contained 64% enzyme capped on AuNPs whereas the remaining 36% enzyme activity is present in supernatant. Moreover, retention of enzymatic activity of such NPs was confirmed by *in vitro* casein agar plate method as well as by *in vivo* anti-inflammatory activity performed in experimental animals. The prepared AuNPs were quite stable for over six month at 25°C. It was demonstrated since there was no shift in surface plasmon band. The use of AuNPs as a carrier for serratiopeptidase exhibited an improvement in its anti-inflammatory activity.

3.2.6. Silicatein. Silicatein is an enzyme used by sponges to capture silicate and build silica nanostructures. The production of controlled nanostructural Ga_2O_3 at low temperature by silicatein has been investigated. This enzyme catalyzed hydrolysis of $\text{Ga}(\text{NO}_3)_3$ into oriented nanocrystallites and it was obtained along the length of filaments in absence of acid or alkali [128]. ZrNPs were produced by incubating fungus *Fusarium oxysporum* with aqueous ZrF_6^{2-} anions; extra-cellular protein-mediated hydrolysis of anionic complexes resulted in the facile room temperature production of nanocrystalline zirconia. Extracellular hydrolysis of metal anions by cationic proteins of molecular weight about 24-28 kDa, which was found catalytically similar to silicatein, was involved in the production of ZrNPs [129]. Andre *et al.* [130] investigated production of nanostructured SnO_2 by silicatein- α . TEM, HRTEM and XRD revealed the formation of cassiterite SnO_2 . Surface bound silicatein retained its catalytic activity. It was demonstrated by immobilizing silicatein on glass surfaces using a histidine-tag chelating anchor. The subsequent deposition of SnO_2 on glass was examined by quartz crystal microbalance measurements and SEM. This aspect of silicatein activity toward the formation of metal oxides other than SiO_2 , TiO_2 and BaTiO_3 demonstrated us new opportunities for the synthesis of composite material.

3.2.7. Trypsin. Trypsin (EC 3.4.21.4) is a serine protease, present in the digestive system of many vertebrates, where it helps in the digestion of proteins. It is synthesized by the pancreas as an inactive precursor, trypsinogen and it is hydrolyzing peptide chains mainly at the carboxyl side of the amino acids lysine or arginine, except when either is followed by proline [131]. It is

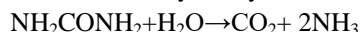
used in several biochemical/biotechnological applications. This enzyme catalyzes the hydrolysis of peptide bonds in proteins in duodenum and produces smaller peptides. The peptide products are then further hydrolyzed into amino acids via other proteases, making them available for absorption into the blood stream. Li and Weng [132] described an eco-friendly approach for synthesis of trypsin-mediated three-dimensional gold nano-flowers with high colloidal stability at room temperature. In this procedure ascorbic acid (AA) was rapidly added into premixed solution of HAuCl_4 and trypsin in a buffer, pH 5.0. The formation of gold nano-flowers involved three steps; i.e., (i) immobilization of AuCl_4^- ions by a positively charged trypsin template, (ii) *insitu* spontaneous reduction of AuCl_4^- ions by AA and capping Au⁰ by 12 cysteine residues of trypsin and (iii) reduction of more AuCl_4^- ions on Au nuclei produced at initial stages and anisotropic growth into gold nano-flowers.

3.2.8. URAK. URAK is a fibrinolytic enzyme produced by *Bacillus cereus* NK1. Deepak *et al.* [133] described an eco-friendly process for the synthesis of silver and gold NPs using purified URAK. The enzyme produced AgNPs when incubated with 1.0 mM AgNO_3 for 24 h and AuNPs when incubated with 1.0 mM HAuCl_4 for 60 h. The addition of NaOH enhanced the production of NPs. AgNPs were produced within 5 min while for the synthesis of AuNPs required 12 h. The synthesized NPs were characterized by a peak at 440 nm and 550 nm in the UV-visible spectrum. TEM analysis showed that the size of silver NPs was 60 nm and AuNPs was 20 nm. XRD confirmed crystalline nature of NPs and AFM demonstrated spherical shape of NPs. The involvement of protein in the synthesis of NPs has been exhibited by FT-IR. Moreover, the synthesized NPs were found to contain immobilized enzyme.

3.3. Other Hydrolases.

3.3.1 Alkaline and acid phosphatases. Kolhatkar *et al.* [134] for the first time described *in vitro* enzymatic synthesis of paramagnetic and antiferromagnetic NPs toward magnetic ELISA reporting. In this method, alkaline phosphatase catalyzed the dephosphorylation of l-ascorbic-2-phosphate, which worked as a reducing agent for salts of iron, gadolinium and holmium, forming magnetic precipitates of $\text{Fe}_{45\pm 14}\text{Gd}_{5\pm 2}\text{O}_{50\pm 15}$ and $\text{Fe}_{42\pm 4}\text{Ho}_{6\pm 4}\text{O}_{52\pm 5}$. The NPs were found to be paramagnetic at 300 K and antiferromagnetic under 25 K. Although weakly magnetic at 300 K, the room-temperature magnetization of the NPs found here is considerably higher as compared to analogous chemically-synthesized $\text{Ln}_x\text{Fe}_y\text{O}_z$ ($\text{Ln} = \text{Gd}, \text{Ho}$) samples discussed earlier. The NPs showed a significantly higher saturation magnetization of 45 and 30 emu g^{-1} for $\text{Fe}_{45\pm 14}\text{Gd}_{5\pm 2}\text{O}_{50\pm 15}$ and $\text{Fe}_{42\pm 4}\text{Ho}_{6\pm 4}\text{O}_{52\pm 5}$ at 5 K, respectively. Thus the procedure of synthesizing magnetic labels reduces the cost and avoids diffusional mass-transfer limitations associated with pre-synthesized magnetic reporter particles. Purple acid phosphatase from *Limonia acidissima* was considered for the synthesis of silver NPs. Stable AgNPs were formed by a sonochemical method using enzyme as a stabilizing and capping agent. UV-vis spectroscopy, FT-IR, XRD and TEM were employed for the characterization of NPs. X-ray study demonstrated that NPs were made of silver and silver oxide. As-prepared NPs showed remarkably high antimicrobial activity against *E. coli*, *P. aeruginosa* and *S. aureus* [135].

3.3.2 Urease. Urease (EC 3.5.1.5) is an enzyme which catalyzes the hydrolysis of urea into CO₂ and NH₃ [136]. The following reaction is catalyzed by urease:



Some workers have investigated urease mediated synthesis of ZnO nanoshells at room temperature. In this work, the urease molecules were incubated with urea and zinc nitrate hexahydrate. Ammonia was produced by the enzyme and ZnO shells were grown on the urease core. The average outer diameter of the nanoshells was 18 nm with a fairly narrow distribution as visualized by TEM. ZnO nanoshells were highly crystalline [137]. Urease was taken to synthesize nanocrystalline TiO₂ and it produced monodisperse TiO₂ nanostructures with high surface area. These nanostructures can be employed in various energy-based applications such as low-cost photovoltaics and photocatalysts [138]. A mechanistic

approach has been developed for the synthesis of metal and metallic alloy NPs by using jack bean urease as a reducing and stabilizing agent under physiological conditions. The urease activity was exploited for the synthesis of metal-ZnO core-shell NC. Thus urease was used as an ideal bionanoreactor for the production of higher order nanostructures such as alloys and core-shell under ambient conditions [139]. Shi *et al.* [104] demonstrated for the first time a simple and environmentally friendly method for the preparation of highly stable dispersions of Fe₃O₄NPs of controlled morphologies by using urease. Fe₃O₄NPs of various morphologies such as nanospheres, nanosheets and nanorods were obtained. The obtained NPs show a larger specific surface area and a stronger magnetism. It increases their dye adsorption capacity and enhances their potential for the treatment of wastewater.

Table 2. Biosynthesis of NM by using carbohydrases.

Name of enzyme	Name of NPs	Size (nm)	Shape	Reference
α-amylase	Au	-	----	[100]
	Au	10-50	----	[101]
α-amylase	AuNPs,	89,86	----	[102, 103]
	AgNPs	37, 37	----	[104]
	Au/Ag alloy NPs	63, 63	----	[105]
	Ag	22-44	Triangular & hexagonal	
	Au	6	Spherical	[107]
TiO ₂	30-55 nm	Monodisperse Nanorings		
Dextranase	CuS	9-27	Nanocrystals	[108]
	Cu ₂ S	14		
	Ag ₂ S	20-50		
	CdS	9		
Endoglucanases	MFC nanofibers	--	Nanofibers	[112] [113]
	MFC nanofibers	Width 30-80 Length 100 nm- 1.8 mm	Nanocrystal	

Table 3. Biosynthesis of NM by Employing Proteases.

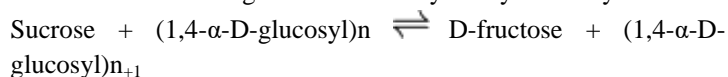
Name of enzyme	Name of NPs	Size (nm)	Shape	Reference
Bacterial protease	Au	----	Rods, cubes, tetrapods & prisms	[117]
R-chymotrypsin	CdS	3	Well dispersed	[119]
Curcain	ZnS	10	Spherical	[121]
Curcain	TiO ₂	25-50	Spherical	[122]
Papain	Au		Fluorescent nanocrystals	[125]
Silicatein	SnO ₂		Cassiterite	[130]
URAK	Ag & Au	60 & 20	Spherical	[133]

4. TRANSFERASE, LYASES AND SYNTHETASES

Table 4 illustrates NPs synthesized by transferases, lyases and synthetases.

4.1. Transferases.

4.1.1. Amylosucrase. Amylosucrase (E.C. 2.4.1.4) is a member of family 13 of the glycoside hydrolases, α-amylases. It also showed biological activity to synthesize amylose-like polymers from sucrose. The following reaction is catalyzed by this enzyme.



The systematic name of this enzyme is sucrose: 1, 4-α-D-glucan 4-α-D-glucosyltransferase. Other commonly used names are

sucrose-glucan glucosyltransferase, and sucrose-1,4-α-glucan glucosyltransferase. This enzyme participates in starch and sucrose metabolism [141]. Lim and coworkers [142] adopted a biological approach to synthesize pure amylose microbeads using amylosucrase from *Deinococcus geothermalis*. Single-walled carbon nanotubes were simply incorporated into amylose structure during enzymatic action in order to produce well-defined amylose-single-walled carbon nanotubes composite microbeads.

4.1.2. Phytochelatinsynthase. Phytochelatinsynthases (EC. 2.3.2.15) are also known as glutathione-γ-glutamyl cysteinyltransferases. These enzymes catalyze synthesis of

phytochelatin and homophytochelatin, the heavy-metal-binding peptides of plants and such enzymes are needed for detoxification of heavy metals, eg., cadmium and arsenate [143]. *E. coli* strains have been genetically engineered to synthesize phytochelatin as capping agents and used for the intracellular synthesis of fluorescent and water-soluble phytochelatin-coated CdS NPs. The size of the semiconductor nanocrystals was controlled by the population of capping phytochelatin [144]. Liu *et al.* [145] synthesized CdS nanocrystals by immobilized phytochelatin synthase which catalyzed conversion of glutathione into metal-binding peptide phytochelatin PC. CdS nanocrystals were produced in the presence of CdCl₂, Na₂S and PC as a capping agent. The highly stable nanocrystals with tunable sizes from 2.0-1.6 nm diameter were synthesized by varying reaction times, different compositions of PCs from PC2 to PC3. It showed that this approach can be generalized to direct *in vitro* self assembly of several nanocrystals of various compositions and sizes. Park *et al.* [146] produced a recombinant *E. coli* system expressing phytochelatin synthase and metallothionein for the synthesis of diverse kinds of metal NPs *in vivo*. The size of the metal NPs was regulated by controlling the concentrations of metal ions. These obtained NPs exhibited good optical, electronic, chemical and magnetic properties.

4.2. Lyases

4.2.1 Cysteine desulphydrase. D-cysteine desulphydrase (EC: 4.4.1.15) catalyses α , β -elimination reaction of D-cysteine and its derivatives.

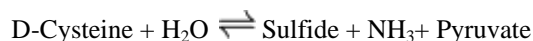


Table 4: Synthesis of NM by Using Transferases, Lyases & Synthetases.

Name of enzyme	Name of NPs	Size (nm)	Shape	Reference
γ -glutamylcysteine synthetase	CdS	--	Nanocrystals	[142]
Phytochelatin synthase	CdS	2-1.6	Nanocrystals	[145]
Cysteine desulphydrase	CdS	8.01+/-0.25	Nanocrystal	[148]
Glutathione synthetase	CdS	2-5	Wurtzite	[150]

5. CONCLUSION

It is concluded that enzymatically synthesized NM are highly safe and suitable for human consumption because their synthesis procedure did not include any additional toxic compound/substance. The as-fabricated NPs have expressed their high antibacterial, antifungal and anticancer activities. However, there are a lot of reservations and a big challenge in using the NM for biomedical and therapeutic uses due to toxicity of the material itself and its impact on the metabolism and structure and functions

6. REFERENCES

- Kaur, A.; Gupta, U. A review on applications of nanoparticles for the preconcentration of environmental pollutants. *J. Mater. Chem.* **2009**, *19*, 8279-8289, <https://doi.org/10.1039/b901933b>.
- Ansari, S.A.; Husain, Q. Potential applications of enzymes immobilized on/in nano materials: A review. *Biotechnol. Adv.* **2012**, *30*, 512-523. <https://doi.org/10.1016/j.biotechadv.2011.09.005>.

This enzyme belongs to the family of lyases, specifically the class of carbon-sulfur lyases. The systematic name of this enzyme is D-cysteine sulfide-lyase (deaminating; pyruvate-forming) [147]. Bai *et al.* [148] have shown the formation of CdS NPs by photosynthetic bacteria *Rhodospseudomonas palustris*. The CdSO₄ solution incubated with *R. palustris* biomass changed into yellow color from 48 h onwards. It exhibited production of CdSNPs and purified solution showed maximum absorbance peak at 425 nm due to CdSNPs in the quantum size regime. X-ray analysis confirmed CdS production and TEM analysis exhibited a uniform distribution of NPs of 8.01+/-0.25 nm whereas electron diffraction pattern confirmed face-centered cubic crystalline structure of CdS. Further, it was noticed that the cysteine desulphydrase producing S(2-) in the *R. palustris* was located in cytoplasm and this cysteine desulphydrase carried out the synthesis of CdS nanocrystal.

4.3. Synthetases

4.3.1. Glutathione synthetase. Glutathione synthetase (GS, EC 6.3.2.3) is one of the enzymes involved in glutathione biosynthesis pathway. It catalyzes the condensation of γ -glutamylcysteine and glycine in presence of ATP in order to synthesize glutathione and ADP [149]. Chen *et al.* [150] constructed a recombinant *E. coli* ABLE C strain to over express GS. The exposure of recombinant cells to CdCl₂ and Na₂S, GS over-expression augmented glutathione synthesis and thus it resulted into the production of CdSNPs. The resultant CdSNPs has wurtzite structure and 2-5 nm size. These findings showed the potential of genetic engineering approach to enhance CdSNPs formation in bacteria.

of biological macromolecules. Prior to applying these nano products as therapeutic agents it is necessary to investigate the effect of NM on the structure and functions of different kinds of biomolecules and biomembranes. To study the toxic effect of such molecules on various organs and organelles of the human body is also necessary before recommending them as nanomedicine or drug.

- Jiang, Y.; Wang, H.; Li, S.; Wen, W. Applications of micro/nanoparticles in microfluidic sensors: A review. *Sensors* **2014**, *14*, 6952-6964, <https://doi.org/10.3390/s140406952>.
- Husain Q.; Magnetic nanoparticles as a tool for the immobilization/stabilization of hydrolases and their applications: An overview. *Biointerfaces Res. Appl. Chem.* **2016**, *6*(6), 1585-1606, <https://doi.org/10.1515/boca-2017-0004>.
- Husain Q.; Nanomaterials as novel support for the immobilization of amylolytic enzymes and their applications: A

- review. *DeGruyterBiocatalysis* **2017**, 3(1), 37-53, doi 10.1515/boca-2017-0004.
6. Husain, Q.; Nanocarriers immobilized proteases and their industrial applications: An overview. *J. Nanosci. Nanotechnol.* **2018**, 18 (1), 486-499, doi: 10.1166/jnn.2018.15246.
7. Rao, C.N.R.; Vivekchand, S.R.C.; Biswasa, K.; Govindaraja, A. Synthesis of inorganic nanomaterials. *Dalton Trans.* **2007**, 14, 3728-3749.
8. Faramarzi, M.A.; Sadighi, A. Insights into biogenic and chemical production of inorganic nanomaterials and nanostructures. *Adv. Coll. Interf. Sci.* **2013**, 189-190, 1-20, <https://doi.org/10.1016/j.cis.2012.12.001>.
9. Khomutov, G.B.; Gubin, S.P. Interfacial synthesis of noble metal nanoparticles. *Mater. Sci. Eng. C* **2002**, 22, 41-146, [https://doi.org/10.1016/S0928-4931\(02\)00162-5](https://doi.org/10.1016/S0928-4931(02)00162-5).
10. Raveendran, P.; Fu, J.; Wallen, S.L. Completely "green" synthesis and stabilization of metal nanoparticles. *J. Am. Chem. Soc.* **2003**, 125, 13940-13941, <https://doi.org/10.1021/ja029267j>.
11. He, B.; Tan, J.; Liew, K.; Liu, H. Synthesis of size controlled Ag nanoparticles. *J. Mol. Catal. A* **2004**, 221, 121-126, <https://doi.org/10.1016/j.molcata.2004.06.025>.
12. Bhattacharya, R.; Saha, S. Growth of CdS nanoparticles by chemical method and its characterization. *Pramana J. Phys.* **2008**, 71, 187-192, <https://doi.org/10.1007/s12043-008-0152-7>.
13. Vithiya, K.; Sen, S. Biosynthesis of nanoparticles. *Int. J. Pharm. Sci. Res.* **2011**, 2, 2781-2785.
14. Korbekandi, H.; Irvani, S.; Abbasi, S. Production of nanoparticles using organisms. *Crit. Rev. Biotechnol.* **2009**, 29, 279-306, <https://doi.org/10.3109/07388550903062462>
15. Irvani, S. Green synthesis of metal nanoparticles using plants. *Green Chem.*, **2011**, 13, 2638-2650, <https://doi.org/10.1039/C1GC15386B>.
16. Irvani, S.; Korbekandi, H.; Mirmohammadi, S.V.; Zolfaghari, B. Synthesis of silver nanoparticles: chemical, physical and biological methods. *Res. Pharm. Sci.*, **2014**, 9, 385-406.
17. Prabhu, S.; Poulose, E.K. Silver nanoparticles: mechanism of antimicrobial action, synthesis, medical applications, and toxicity effects. *Inter. Nano Lett.* **2012**, 2, 32, <http://dx.doi.org/10.1186/2228-5326-2-32>.
18. Kulkarni, N.; Muddapur, U. Biosynthesis of metal nanoparticles: A review. *J. Nanotechnol.* **2014**, <http://dx.doi.org/10.1155/2014/510246>.
19. Li, X.; Xu, H.; Chen, Z.-S.; Chen, G. Biosynthesis of nanoparticles by microorganisms and their applications. *J. Nanomater.* **2011**, <http://dx.doi.org/10.1155/2011/270974>.
20. Kshatriya, R.B.; Shaikh, Y.I.; Nazeruddin, G.M. Synthesis of green metallic nanoparticles (NPs) and applications. *Orient. J. Chem.*, **2013**, 29, 1589-1595, <http://dx.doi.org/10.13005/ojc/290442>.
21. Sunkar, S.; Nachiyar, C.V. Endophytic fungi mediated extracellular silver nanoparticles as effective antibacterial agents. *Int. J. Pharm. Pharm. Sci.* **2013**, 5, 95-100.
22. Khan, M.J.; Qayyum, S.; Husain, Q.; Alam, F. Effect of tin oxide nanoparticles binding on the structure and activity of α -amylase from *Bacillus amyloliquefaciens*. *Nanotechnology* **2011**, 22, <https://doi.org/10.1088/0957-4484/22/45/455708>.
23. Ansari, S.A.; Husain, Q. Immobilization of *Kluyveromyces lactis* beta-galactosidase on concanavalin A layered aluminium oxide nanoparticles-its future aspects in biosensor applications. *J. Mol. Catal. B: Enzym.*, **2011**, 70, 119-126, <https://doi.org/10.1016/j.molcatb.2011.02.016>.
24. Ansari, S.A.; Husain, Q.; Qayyum, S.; Azam, A. Designing and surface modification of zinc oxide nanoparticles for biomedical applications. *Food Chem. Toxicol.*, **2011**, 49, 2107-2115, <https://doi.org/10.1016/j.fct.2011.05.025>.
25. Schneidewind, H.; Schüller, T.; Strelau, K.K.; Weber, K.; Cialla, D.; Diegel, M.; Mattheis, R.; Berger, A.; Möller, R.; Popp, J. The morphology of silver nanoparticles prepared by enzyme-induced reduction. *Beilstein J. Nanotechnol.* **2012**, 3, 404-414, <https://dx.doi.org/10.3762%2Fbjnano.3.47>.
26. Husain, Q. High Yield immobilization and stabilization of oxidoreductases using magnetic nanosupports and their potential applications: an update. *Current Catal.* **2017**, 6(3), 168-187, [10.2174/2211544706666170704141828](https://doi.org/10.2174/2211544706666170704141828)
27. Jha, A.K.; Prasad, K.; Prasad, K. A green low-cost biosynthesis of Sb₂O₃ nanoparticles. *Biochem. Eng. J.*, **2009**, 43, 303-306, <https://doi.org/10.1016/j.bej.2008.10.016>.
28. Jha, A.K.; Prasad, K.A.R.; Kulkarni, A.R. Synthesis of TiO₂ nanoparticles using microorganisms. *Coll. Surf. B: Biointerf.* **2009**, 71, 226-229, <https://doi.org/10.1016/j.colsurfb.2009.02.007>.
29. Jayaseelan, C.; Rahuman, A.A.; Kirthi, A.V.; Marimuthu, S.; Santhoshkumar, T.; Bagavan, A.; Gaurav, K.; Karthik, L.; Bhaskara Rao, K.V.B. Novel microbial route to synthesize ZnO nanoparticles using *Aeromonas hydrophila* and their activity against pathogenic bacteria and fungi. *Spect. Acta Part A: Mol. Biomol. Spec.* **2012**, 90, 78-84, <https://doi.org/10.1016/j.saa.2012.01.006>.
30. Sandana, N.J.G.; Rose, C. Facile production of ZnS quantum dot nanoparticles by *Saccharomyces cerevisiae* MTCC 2918. *J. Biotechnol.*, **2014**, 170, 73-78, <https://doi.org/10.1016/j.jbiotec.2013.11.017>.
31. Jan, U.; Husain, Q.; Saleemuddin, M. Preparation of stable, highly active and immobilized glucose oxidase using the anti-enzyme antibodies and F(ab)₂. *Biotechnol. Appl. Biochem.* **2001**, 34, 13-17, <https://doi.org/10.1042/BA20010011>.
32. Jan, U.; Husain, Q. Preparation of highly stable, very active and high yield multilayered assembly of glucose oxidase by using carbohydrate specific polyclonal antibodies. *Biotechnol. Appl. Biochem.* **2004**, 39, 233-239, <https://doi.org/10.1042/BA20030092>.
33. Bankar, S.B.; Bule, M.V.; Singhal, R.S.; Ananthanarayan, L. Glucose oxidase-An overview. *Biotechnol. Adv.* **2009**, 27, 489-501, <https://doi.org/10.1016/j.biotechadv.2009.04.003>.
34. Yasui, K.; Kimizuka, N. Enzymatic synthesis of gold nanoparticles wrapped by glucose oxidase. *Chem. Lett.* **2005**, 34, 416-417, <https://doi.org/10.1246/cl.2005.416>.
35. Caseli, L.; dos Santos Jr.D.S.; Aroca, R.F.; Oliveira Jr.O.N. Controlled fabrication of gold nanoparticles biomediated by glucose oxidase immobilized on chitosan layer-by-layer films. *Mate. Sci. Eng: C*, **2009**, 29, 1687-1690, <https://doi.org/10.1016/j.msec.2009.01.013>.
36. Meister, A. Glutathione metabolism and its selective modification. *J. Biol. Chem.* **1988**, 263, 17205-17208.
37. Scott, D.M. *Enzyme catalyzed metallic nanoparticle synthesis and the electrochemical characterization of the glutathione reductase-gold nanoparticle complex*. Press University of California Davis, 2006.
38. Scott, D.; Toney, M.; Muzikár, M. Harnessing the mechanism of glutathione reductase for synthesis of active site bound metallic nanoparticles and electrical connection to electrodes. *J. Am. Chem. Soc.* **2008**, 130, 865-874, <https://doi.org/10.1021/ja074660g>.
39. Pugin, B.; Cornejo, F.A.; Muñoz-Díaz, P.; Muñoz-Villagrán, C.M.; Vargas-Pérez, J.I.; Arenas, F.A.; Vásquez, C.C. Glutathione

- reductase-mediated synthesis of tellurium-containing nanostructures exhibiting antibacterial properties. *Appl. Environ. Microbiol.* **2014**, *80*, 7061-7070, <https://doi.org/10.1128/AEM.02207-14>.
40. Ruzhenikov, S.N.; Burke, J.; Sedelnikova, S.; Baker, P. J.; Taylor, R.; Bullough, P.A.; Muir, N.M.; Gore, M.G.; Rice, D.W. Glycerol dehydrogenase. *Structure* **2001**, *9*, 789-802.
41. Niide, T.; Kamiya, N. Biocatalytic synthesis of gold nanoparticles with cofactor regeneration in recombinant *Escherichia coli* cells. *Chem. Commun. (Camb)* **2011**, *47*, 7350-7352, <https://doi.org/10.1039/C1CC12302E>.
42. Fontecilla-Camps, J.C.; Volbeda, A.; Cavazza, C.; Nicolet, Y. Structure/function relationships of [NiFe]- and [FeFe]-hydrogenases. *Chem. Rev.* **2007**, *107*, 4273-4303, <https://doi.org/10.1021/cr050195z>.
43. Riddin, T.L.; Yageshni, G.; Gericke, M.; Whiteley, C.G. Two different hydrogenase enzymes from sulphate-reducing bacteria are responsible for the bioreductive mechanism of platinum into nanoparticles. *Enzyme Microb. Technol.* **2009**, *45*, 267-273, <https://doi.org/10.1016/j.enzmictec.2009.06.006>.
44. Govender, Y.; Riddin, T.L.; Gericke, M.; Whiteley, C.G. On the enzymatic formation of platinum nanoparticles. *J. Nanopart. Res.* **2010**, *12*, 261-271, <https://doi.org/10.1007/s11051-009-9604-3>.
45. Riddin, T.L. *Investigating the enzymatic mechanism of platinum nanoparticle synthesis in sulfate-reducing bacteria*. Masters Thesis, Rhodes University, Deposited On 15 Mar 2012.
46. Claus, H. Laccases: Structure, reactions, distribution. *Micron* **2004**, *35*, 93-96, <https://doi.org/10.1016/j.micron.2003.10.029>.
47. Alcalde, M. Laccases: Biological functions, molecular structure and industrial applications. In *J. Polaina & A.P. MacCabe (Eds.), Industrial Enzymes*, 2007; pp. 461-476. https://doi.org/10.1007/1-4020-5377-0_26.
48. Galliker, P., Hommes, G., Schlosser, D., Philippe F.-X. Corvini, P.F.X. & Shahgaldian, P. Laccase-modified silica nanoparticles efficiently catalyze the transformation of phenolic compounds. *J. Coll. Interf. Sci.* **2010**, *349*, 98-105, <https://doi.org/10.1016/j.jcis.2010.05.031>.
49. Sanghi, R.; Verma, P.; Puri, S. Enzymatic formation of gold nanoparticles using *Phanerochaete chrysosporium*. *Adv. Chem. Eng. Sci.* **2011**, *1*, 154-162, <https://doi.org/10.4236/aces.2011.13023>.
50. Faramarzi, M.A.; Forootanfar, H. Biosynthesis and characterization of gold nanoparticles produced by laccase from *Paraconiothyrium variabile*. *Coll. Surf. B: Bioint.* **2011**, *87*, 23-27, <https://doi.org/10.1016/j.colsurfb.2011.04.022>.
51. Vetchinkina, E.P.; Loshchinina, E.A.; Burov, A.M.; Dykman, L.A.; Nikitina, V.E. Enzymatic formation of gold nanoparticles by submerged culture of the basidiomycete *Lentinus edodes*. *J. Biotechnol.* **2014**, *182-183*, 37-45, <https://doi.org/10.1016/j.jbiotec.2014.04.018>.
52. Coquelle, N.; Fioravanti, E.; Weik, M.; Vellieux, F.; Madern, D. Activity, stability and structural studies of lactate dehydrogenases adapted to extreme thermal environments. *J. Mol. Biol.* **2007**, *374*, 547-562, <https://doi.org/10.1016/j.jmb.2007.09.049>.
53. Oza, G.; Pandey, S.; Sharon, M. Extracellular biosynthesis of gold nanoparticles using *Escherichia coli* and deciphering: The role of lactate dehydrogenase using Ldh knock out *E. Coli*. *J. Atom. Mol.* **2012**, *2*, 301-311.
54. Lin, H. Nicotinamide adenine dinucleotide: Beyond a redox coenzyme. *Org. Biomol. Chem.* **2007**, *5*, 2541-2554, <http://dx.doi.org/10.1039/B706887E>.
55. Dudev, T.; Lim, C. Factors controlling the mechanism of NAD⁺ non-redox reactions. *J. Am. Chem. Soc.* **2010**, *132*, 16533-16543, <https://doi.org/10.1021/ja106600k>.
56. Kathiresan, K.; Manivannan, S.; Nabeel, M.A.; Dhivya, B. Studies on silver nanoparticles synthesized by a marine fungus, *Penicillium fellutanum* isolated from coastal mangrove sediment. *Coll. Surf. B* **2009**, *71*, 133-137, <https://doi.org/10.1016/j.colsurfb.2009.01.016>.
57. Li, G.; He, D.; Qian, Y.; Guan, B.; Gao, S.; Cui, Y.; Yokoyama, K.; Wang, L. Fungus-mediated green synthesis of silver nanoparticles using *Aspergillus terreus*. *Int. J. Mol. Sci.* **2012**, *13*, 466-476, <https://doi.org/10.3390/ijms13010466>.
58. Correa-Llantén, D.N.; Muñoz-Ibacache, S.A.; Castro, M.E.; Muñoz, P. A.; Jenny, M.; Blamey, M. Gold nanoparticles synthesized by *Geobacillus* sp. strain ID17 a thermophilic bacterium isolated from Deception Island, Antarctica. *Microb. Cell Fact.* **2013**, *12*, 75, <https://doi.org/10.1186/1475-2859-12-75>.
59. He, S.; Guo, Z.; Zhang, Y.; Zhang, S.; Wang, J.; Gu, N. Biosynthesis of gold nanoparticles using the bacteria *Rhodospseudomonas capsulate*. *Mater. Lett.* **2007**, *61*, 3984-3987, <https://doi.org/10.1016/j.matlet.2007.01.018>.
60. Lederer, F. Cytochrome b5 fold-an adaptable module. *Biochimie* **1994**, *76*, 674-692, [https://doi.org/10.1016/0300-9084\(94\)90144-9](https://doi.org/10.1016/0300-9084(94)90144-9).
61. Durán, N.; Marcato, P.D.; Alves, O.L.; DeSouza, G.I.H.; Esposito, E. Mechanistic aspects of biosynthesis of silver nanoparticles by several *Fusarium oxysporum* strains. *J. Nanobiotechnol.* **2005**, *3*, 8, <https://doi.org/10.1186/1477-3155-3-8>.
62. Kumar, S.A.; Abyaneh, M.K.; Gosavi, S.W.; Kulkarni, S.K.; Pasricha, R.; Ahmad, A.; Khan, M.I. Nitrate reductase-mediated synthesis of silver nanoparticles from AgNO₃. *Biotechnol. Lett.* **2007**, *29*, 439-445, <https://doi.org/10.1007/s10529-006-9256-7>.
63. Basavaraja S.; Balaji S.D.; Lagashetty A.; Rajasab A.H.; Venkataraman A. Extracellular biosynthesis of silver nanoparticles using the fungus *Fusarium semitectum*. *Mater. Res. Bull.* **2008**, *43*, 1164-1170, <https://doi.org/10.1016/j.materresbull.2007.06.020>.
64. Patil, S.R. Antibacterial activity of silver nanoparticles from *Fusarium semitectum*. *CIB Tech. J. Biotechnol.* **2014**, *3*, 8-12.
65. Vaidyanathan, R.; Gopalram, S.; Kalishwaralal, K.; Deepak, V.; Pandian, S.R.; Gurunathan, S. Enhanced silver nanoparticle synthesis by optimization of nitrate reductase activity. *Coll. Surf. B Bioint.* **2010**, *75*, 335-341, <https://doi.org/10.1016/j.colsurfb.2009.09.006>.
66. Oza, G.; Pandey, S.; Shah, R.; Sharon, M. A mechanistic approach for biological fabrication of crystalline gold nanoparticles using marine algae *Sargassum wightii*. *Eur. J. Exper. Biol.* **2012**, *2*, 505-512.
67. Pandey, S.; Oza, G.; Kalita, G.; Sharon, M. *Adathoda vasica*-an intelligent fabricator of gold nanoparticles. *Eur. J. Exp. Biol.* **2012**, *2*, 468-474.
68. Pandey, S.; Oza, G.; Gupta, A.; Shah, R.; Sharon, M. The possible involvement of nitrate reductase from *Asparagus racemosus* in biosynthesis of gold nanoparticles. *Eur. J. Exp. Biol.* **2012**, *2*, 475-483.
69. El-Batal, A.I.; Amin, M.A.; Shehata, M.M.K.; Hallol, M.M.A. Synthesis of silver nanoparticles by *Bacillus stearothermophilus* using gamma radiation and their antimicrobial activity. *World Appl. Sci. J.* **2013**, *22*, 1-16.
70. Nithya, R.; Ragnathan, R. Synthesis of silver nanoparticles using a probiotic microbe and its antibacterial effect against multidrug resistant bacteria. *Afr. J. Biotechnol.* **2012**, *11*, 11013-11021.

71. Mewada, A.; Oza, G.; Pandey, S.; Sharon, M. Extracellular synthesis of gold nanoparticles using *Pseudomonas denitrificans* and comprehending its stability. *J. Microbiol. Biotech. Res.* **2012**, *2*, 493-499.
72. Prakash, U.R.T.; Thiagarajan, P. Syntheses and characterization of silver nanoparticles using *Penicillium* sp. isolated from soil. *Int. J. Adv. Sci. Tech. Res.* **2012**, *1*, 137-149.
73. Gunasekar, V.; Divya, B.; Brinda, K.; Vijaykrishnan, J.; Ponnusami, V.; Rajan, K.S. Enzyme mediated synthesis of Ag-TiO₂ photocatalyst for visible light degradation of reactive dye from aqueous solution. *J. Sol-Gel Sci. Technol.* **2013**, *68*, 60-66, <https://doi.org/10.1007/s10971-013-3134-2>.
74. Fernando, L.M.; Merca, F.E.; Paterno, E.S. Biogenic synthesis of gold nanoparticles by plant-growth-promoting bacteria isolated from Philippine soils. *Philipp. Agric. Sci.* **2013**, *96*, 129-136.
75. Lin, I.W.S.; Lok, C.N.; Che, C.M. Biosynthesis of silver nanoparticles from silver(I) reduction by the periplasmic nitrate reductase c-type cytochrome subunit NapC in a silver-resistant *E. coli*. *Chem. Sci.* **2014**, *5*, 3144-3150, <http://dx.doi.org/10.1039/c4sc00138a>.
76. Gholami-Shabani, M.; Akbarzadeh, A.; Norouzi, D.; Amini, A.; Gholami-Shabani, Z.; Imani, A.; Chiani, M.; Riazi, G.; Shams-Ghahfarokhi, M.; Razzaghi-Abyaneh, M. Antimicrobial activity and physical characterization of silver nanoparticles green synthesized using nitrate reductase from *Fusarium oxysporum*. *Appl. Biochem. Biotechnol.* **2014**, *172*, 4084-4098, <https://doi.org/10.1007/s12010-014-0809-2>.
77. Veitch, N.C. Structural determinants of plant peroxidase function. *Phytochem. Rev.* **2004**, *3*, 3-18, <https://doi.org/10.1023/B:PHYT.0000047799.17604.94>.
78. Fatima, A.; Husain, Q. Purification and characterization of a novel peroxidase from bitter melon (*Momordica charantia*). *Protein Peptide Lett.* **2008**, *15*, 377-384, <https://doi.org/10.2174/092986608784246452>.
79. Thiagarajan, M.; Kumar, J.; Samuelson, L.A.; Cholli, A.L. Enzymatically synthesized conducting polyaniline nanocomposites: A solid state NMR study. *J. Macromol. Sci.: Part A Pure Appl. Chem.* **2003**, *A 40*, 1347-1355, <https://doi.org/10.1081/MA-120025314>.
80. Nickels, P.; Dittmer, W.U.; Beyer, S.; Kotthaus, J.P.; Simmel, F.C. Polyaniline nanowire synthesis templated by DNA. *Nanotechnology* **2004**, *15*, 1524, <https://doi.org/10.1088/0957-4484/15/11/026>.
81. Cholli, A.L.; Thiagarajan, M.; Kumar, J.; Parmar, V.S. Biocatalytic approaches for synthesis of conducting polyaniline nanoparticles. *Pure Appl. Chem.* **2005**, *77*, 339-344, <https://doi.org/10.1351/pac200577010339>.
82. Trakhtenberg, S.; Hangan-Balkir, Y.; Warner, J.C.; Bruno, F.F.; Kumar, J.; Nagarajan, R.; Samuelson, L.A. Photo-cross-linked immobilization of polyelectrolytes for enzymatic construction of conductive nanocomposites. *J. Am. Chem. Soc.* **2005**, *127*, 9100-9104, <https://doi.org/10.1021/ja042438v>.
83. Cruz-Silva, R.; Escamilla, A.; Nicho, M.E.; Padron, G.; Ledezma-Perez, A.; Arias-Marin, E.; Ivana Moggio, I.; Romero-Garcia, J. Enzymatic synthesis of pH-responsive polyaniline colloids by using chitosan as steric stabilizer. *Europ. Polym. J.* **2007**, *43*, 3471-3479, <https://doi.org/10.1016/j.eurpolymj.2007.05.027>.
84. Nabid, M.R.; Golbabaee, M.; Moghaddam, A.B.; Dinarvand, R.; Sedghi, R. Polyaniline/TiO₂ nanocomposite: Enzymatic synthesis and electrochemical properties. *Int. J. Electrochem. Sci.* **2008**, *3*, 1117-1126.
85. Gao, L.; Wu, J.; Gao, D. Enzyme-controlled self-assembly and transformation of nanostructures in a tetramethylbenzidine/horseradish peroxidase/H₂O₂ system. *ACS Nano*, **2011**, *5*, 6736-6742, <https://doi.org/10.1021/nn2023107>.
86. Ryu, K.; Xue, H.; Park, J. Benign enzymatic synthesis of multiwalled carbon nanotube composites uniformly coated with polypyrrole for supercapacitors. *J. Chem. Technol. Biotechnol.* **2013**, *88*, 788-793, <https://doi.org/10.1002/jctb.3899>.
87. Nabid, M.R.; Shamsianpour, M.; Sedghi, R.; Moghaddam, A.B. Enzyme-catalyzed synthesis of conducting polyaniline nanocomposites with pure and functionalized carbon nanotubes. *Chem. Eng. Technol.* **2012**, *35*, 1707-1712, <https://doi.org/10.1002/ceat.201100149>.
88. Guerrero-Bermea, C.; Sepulveda-Guzman, S.; Cruz-Silva, R. Enzymatic synthesis of polyaniline/graphite oxide nanocomposites. *MRS Proc.* **2012**, *1448*, <https://doi.org/10.1557/opl.2012.1493>.
89. Nguyen, T.P.; Doan, B.H.P.; Dang, D.V.; Nguyen, C.K.; Tran, N.Q. Enzyme-mediated *in situ* preparation of biocompatible hydrogel composites from chitosan and biphasic calcium phosphate nanoparticles for bone regeneration. *Adv. Nat. Sci.: Nanosci. Nanotechnol.* **2014**, *5*.
90. Pinto, R.; Harrison, J.S.; Hsu, T.; Jacobs, W.R.; Leyh, T.S. Sulfite reduction in Mycobacteria. *J. Bacteriol.* **2007**, *189*, 6714-6722, <https://dx.doi.org/10.1128/JB.00487-07>.
91. Parey, K.; Warkentin, E.; Kroneck, P.M.; Ermler, U. Reaction cycle of the dissimilatory sulfite reductase from *Archaeoglobus fulgidus*. *Biochemistry*, **2010**, *49*, 8912-8921, <http://dx.doi.org/10.1021/bi100781f>.
92. Ahmad, A.; Mukherjee, P.; Mandal, D.; Senapati, S.; Khan, M.I.; Kumar, R.; Sastry, M. Enzyme mediated extracellular synthesis of CdS nanoparticles by the fungus *Fusarium oxysporum*. *J. Am. Chem. Soc.* **2002**, *124*, 12108-12109, <https://doi.org/10.1021/ja027296o>.
93. Ansary, A.A.; Kumar, S.A.; Krishnasastri, M.V.; Abyaneh, M.K.; Kulkarni, S.K.; Ahmad, A.; Khan, M.I. CdS quantum dots: Enzyme mediated *in vitro* synthesis, characterization and conjugation with plant lectins. *J. Biomed. Nanotechnol.* **2007**, *3*, 406-413, <https://doi.org/10.1166/jbn.2007.045>.
94. Kumar, S.A.; Abyaneh, M.K.; Gosavi, S.W.; Kulkarni, S.K.; Ahmad, A.; Khan, M.I. Sulfite reductase-mediated synthesis of gold nanoparticles capped with phytochelatin. *Biotechnol. Appl. Biochem.* **2007**, *47*, 191-195, <https://doi.org/10.1042/BA20060205>.
95. Ansary, A.A.; Khan, M.I.; Gaikwad, S.M. *In vitro* enzyme mediated synthesis of metal sulfide nanoparticles: Control of particle size of CdS, Ni₇S₆, PbS, Co₃S₄ nanoparticles using synthetic peptides. *Sci. Adv. Mater.* **2012**, *4*, 179-186, <https://doi.org/10.1166/sam.2012.1270>.
96. Khan, S.A.; Ahmad, A. Enzyme mediated synthesis of water-dispersible, naturally protein capped, monodispersed gold nanoparticles; their characterization and mechanistic aspects. *RSC Adv.* **2014**, *4*, 7729-7734, <https://doi.org/10.1039/C3RA43888K>.
97. Gholami-Shabani, M.; Shams-Ghahfarokhi, M.; Gholami-Shabani, Z.; Azbarzadeh, A.; Riazi, G.; Adjari, S.; Razzaghi-Abyaneh, M. Enzymatic synthesis of gold nanoparticles using sulfite reductase purified from *Escherichia coli*: A green eco-friendly approach. *Process Biochem.* **2015**, *50*, 1076-1085, <https://doi.org/10.1016/j.procbio.2015.04.004>.
98. Gholami-Shabani, M.; Imani, A.; Shams-Ghahfarokhi, M.; Gholami-Shabani, Z.; Pazooki, A.; Azbarzadeh, A.; Riazi, G.;

- Razzaghi-Abyaneh, M. Bioinspired synthesis, characterization and antifungal activity of enzyme-mediated gold nanoparticles using a fungal oxidoreductase. *J. Iran. Chem. Soc.* **2016**, *13*, 2059-2068, <https://doi.org/10.1007/s13738-016-0923-x>.
99. Khan, M.J.; Husain, Q.; Azam, A. Immobilization of porcine pancreatic α -amylase on magnetic Fe₂O₃ nanoparticles: Applications to the hydrolysis of starch. *Biotechnol Bioprocess Eng.* **2012**, *17*(2), 377-384.
100. Rangnekar, A.; Sarma, T.K.; Singh, A.K.; Deka, J.; Ramesh, A.; Chattopadhyay, A. Retention of enzymatic activity of α -amylase in the reductive synthesis of gold nanoparticles. *Langmuir* **2007**, *23*, 5700-5706, <https://doi.org/10.1021/la062749e>.
101. Kalishwaralal, K.; Gopalram, S.; Vaidyanathan, R.; Deepak, V.; Pandian, S.R.; Gurunathan, S. Optimization of α -amylase production for the green synthesis of gold nanoparticles. *Coll. Surf. B Bioint.* **2010**, *77*, 174-180, <https://doi.org/10.1016/j.colsurfb.2010.01.018>.
102. Moshfegh, M.; Forootanfar, H.; Zare, B.; Shahverdi, A.R.; Zarrini, G.; Faramarzi, M.A. Biological synthesis of Au, Ag & Au-Ag biometallic nanoparticles by α -amylase. *Digest J. Nanomat. Biostr.* **2011**, *6*, 1419.
103. Mousavi, S., Forootanfar, H., Faramarzi, M., Ameri, A. & Shakibaie, M. Metal nanoparticle production assisted by α -amylase. *Res. Pharm. Sci.* **2012**, *7*, 218.
104. Mishra, A.; Sardar, M. α -Amylase mediated synthesis of silver nanoparticles. *Sci. Adv. Mater.* **2012**, *4*, 143-146, <https://doi.org/10.1166/sam.2012.1263>.
105. Arunkumar, P.; Thanalakshmi, M.; Kumar, P.; Premkumar, K. *Micrococcus luteus* mediated dual mode synthesis of gold nanoparticles: Involvement of extracellular α -amylase and cell wall teichuronic acid. *Coll. Surf. B: Bioint.* **2013**, *103*, 517-522, <https://doi.org/10.1016/j.colsurfb.2012.10.051>.
106. Mishra, A.; Sardar, M. Alpha amylase mediated synthesis of gold nanoparticles and their application in the reduction of nitroaromatic pollutants. *Energy Environ Focus* **2014**, *3*, 179-184, <https://doi.org/10.1166/eef.2014.1077>.
107. Ahmad, R.; Mohsin, M.; Ahmad, T.; Sardar, M. Alpha amylase assisted synthesis of TiO₂ nanoparticles: Structural characterization and application as antibacterial agents. *J. Hazard. Mater.* **2015**, *283*, 171-177, <https://doi.org/10.1016/j.jhazmat.2014.08.073>.
108. Kim, Y.Y.; Walsh, D. Metal sulfide nanoparticles synthesized via enzyme treatment of biopolymer stabilized nanosuspensions. *Nanoscale*, **2010**, *2*, 240-247, <https://doi.org/10.1039/b9nr00194h>.
109. Ahmed, F.; Qayyum, S.; Husain, Q. Benign nano-assemblages of silver induced by β galactosidase with augmented antimicrobial and industrial dye degeneration potential. *Mater. Sci. Eng. C.* **2018**, *91*, 570-578, <https://doi.org/10.1016/j.msec.2018.05.077>.
110. Bharimalla, A.K., Deshmukh, S.P., Vigneshwaran, N., Patil P.G., Prasad, V. Nanocellulose polymer composites for applications in food packaging: Current status, future prospects and challenges. *Polym. Plastic. Technol. Eng.* **2017**, *56*, 805-823, <https://doi.org/10.1080/03602559.2016.1233281>.
111. Karim, Z.; Afrin, S.; Husain, Q.; Danish, R. Necessity of enzymatic hydrolysis for production and functionalization of nanocelluloses. *Crit. Rev. Biotechnol.* **2017**, *37*, 355-370, <https://doi.org/10.3109/07388551.2016.1163322>.
112. Henriksson, M.; Henriksson, G.; Berglund, L.A.; Lindstrom, T. An environmentally friendly method for enzyme-assisted preparation of microfibrillated cellulose (MFC) nanofibers. *Eur. Polym. J.* **2007**, *43*, 3434-3441.
113. Filson, P.B.; Dawson-Andoha, B.E.; Schwegler-Berry, D. Enzymatic-mediated production of cellulose nanocrystals from recycled pulp. *Green Chem.* **2009**, *11*, 1808-1814, <https://doi.org/10.1039/B915746H>.
114. George, J.; Ramana, K.V.; Bawa, A.S.; Siddaramaiah. Bacterial cellulose nanocrystals exhibiting high thermal stability and their polymer nanocomposites. *Int. J. Biol. Macromol.* **2011**, *48*, 50-57, <https://doi.org/10.1016/j.ijbiomac.2010.09.013>.
115. Zhang, Y.; Lu, X-B.; Gao, C.; Lv, W-J.; Yao, J-M. Preparation and characterization of nano crystalline cellulose from bamboo fibers by controlled cellulase hydrolysis. *J. Fib. Bioeng. Inform.* **2012**, *5*, 263-271.
116. Anderson, S.R.; Esposito, D.; Gillette, W.; Zhu, J.Y.; Baxa, U.; Mcneil, S.E. Enzymatic preparation of nanocrystalline and microcrystalline cellulose. *Tappi J.* **2014**, *13*, 35-42.
117. Bharde, A.; Kulkarni, A.; Rao, M.; Prabhune, A.; Sastry, M. Bacterial enzyme mediated biosynthesis of gold nanoparticles. *J. Nanosci. Nanotechnol.* **2007**, *7*, 4369-4377.
118. Petsko, G.; Ringe, D. Protein structure and function. Oxford: Oxford University Press, 2009; pp.78-79.
119. Narayanan, S.S.; Sarkar, R.; Pal, S.K. Structural and functional characterization of enzyme-quantum dot conjugates: covalent attachment of CdS nanocrystal to r-chymotrypsin. *J. Phys. Chem. C* **2007**, *111*, 11539-11543, <https://doi.org/10.1021/jp072636j>.
120. Devappa, R.K.; Makkar, H.P.S.; Becker, K. Nutritional, biochemical and pharmaceutical potential of proteins and peptides from *Jatropha*: review. *J. Agric. Food. Chem.* **2010**, *58*, 6543-6555.
121. Hudlikar, M.; Joglekar, S.; Dhaygude, M.; Kodam, K. Green synthesis of TiO₂ nanoparticles by using aqueous extract of *Jatropha curcas* L. latex. *Mater. Lett.* **2012**, *75*, 196-199, <https://doi.org/10.1016/j.matlet.2012.02.018>.
122. Hudlikar, M.; Joglekar, S.; Dhaygude, M.; Kodam, K. Latex-mediated synthesis of ZnS nanoparticles: green synthesis approach. *J. Nanopart. Res.* **2012**, *14*, 865, <https://doi.org/10.1007/s11051-012-0865-x>.
123. Lopes, M.C.; Mascarini, R.C.; da Silva, B.M.; Flório, F.M.; Basting, R.T. Effect of a papain-based gel for chemo-mechanical caries removal on dentin shear bond strength. *J. Dent. Child (Chic)* **2007**, *74*, 93-97.
124. Paul, B.; Nasreen, M.; Sarker, A.; Islam, M.R. Isolation, purification and modification of papain enzyme to ascertain industrially valuable nature. *Int. J. Biotechnol. Res.* **2013**, *3*, 11-22.
125. Wang, C. Y.; Wang, C.; Li W.; Zhou, H.; Jiao, H.; Lin, Q.; Yu, C. Papain-directed synthesis of luminescent gold nanoclusters and the sensitive detection of Cu²⁺. *J. Coll. Interf. Sci.* **2013**, *396*, 63-68, <https://doi.org/10.1016/j.jcis.2013.01.031>.
126. Bhagat, S.; Agrawal, M.; Roy, V. Serratiopeptidase: A systematic review of the existing evidence. *Int. J. Surg.* **2013**, *11*, 209-217, <https://doi.org/10.1016/j.ijsu.2013.01.010>.
127. Venkatpurwar, V.P.; Pokharkar, V.B. Biosynthesis of gold nanoparticles using therapeutic enzyme: *in-vitro* and *in-vivo* efficacy study. *J. Biomed. Nanotechnol.* **2010**, *6*, 667-674, <https://doi.org/10.1166/jbn.2010.1163>.
128. Kisailus, D.; Choi, J.H.; Weave, J.C.; Yang, W.; Morse, D.E. Enzymatic synthesis and nanostructural control of gallium oxide at low temperature. *Adv. Mater.* **2005**, *17*, 314-18, <https://doi.org/10.1002/adma.200400815>.
129. Bansal, V.; Rautaray, D.; Ahmad, A.; Sastry, M. Biosynthesis of zirconia nanoparticles using the fungus

- Fusariumoxysporum*. *J. Mater. Chem.* **2004**, *14*, 3303-3305, <https://doi.org/10.1039/B407904C>.
130. André, R.; Tahir, M.N.; Schröder, H.C.C.; Müller, W.E.G.; Tremel, W. Enzymatic synthesis and surface deposition of tin dioxide using silicatein- α . *Chem. Mater.* **2011**, *23*, 5358-5365, <https://doi.org/10.1021/cm201977c>.
131. Leiros, H.K.; Brandsdal, B.O.; Andersen, O.A.; Os, V.; Leiros, I.; Helland, R.; Otlewski, J.; Willassen, N.P.; Smalås, A.O. Trypsin specificity as elucidated by LIE calculations, X-ray structures, and association constant measurements. *Protein Sci.* **2004**, *13*, 1056-1070, <https://doi.org/10.1110/ps.03498604>.
132. Li, L.; Weng, J. Enzymatic synthesis of gold nanoflowers with trypsin. *Nanotechnology*, **2010**, *21*, <https://doi.org/10.1088/0957-4484/21/30/305603>.
133. Deepak, V.; Umamaheshwaran, P.S.; Guhan, K.; Nanthini, R.A.; Krithiga B.; Jaithoon N.M.; Gurunathan, S. Synthesis of gold and silver nanoparticles using purified URAK. *Coll. Surf. B Bioint.* **2011**, *86*, 353-358, <https://doi.org/10.1016/j.colsurfb.2011.04.019>.
134. Kolhatkar, A.G.; Dannongoda, C.; Kourentzi, K.; Jamison, A.C.; Nekrashevich, I.; Kar, A.; Cacao, E.; Strych, U.; Rusakova, I.; Martirosyan, K.S.; Litvinov, D.; Lee, T.R.; Willson, R.C. Enzymatic synthesis of magnetic nanoparticles. *Int. J. Mol. Sci.* **2015**, *16*, 7535-7550, <https://doi.org/10.3390/ijms16047535>.
135. Pawar, O.; Deshpande, N.; Dagade, S.; Waghmode S.; Joshi, P.N. Green synthesis of silver nanoparticles from purple acid phosphatase apoenzyme isolated from a new source *Limonia acidissima*. *J. Exp. Nanosci.* **2016**, *11*, 28-37, <https://doi.org/10.1080/17458080.2015.1025300>.
136. Zimmer, M. Molecular mechanics evaluation of the proposed mechanisms for the degradation of urea by urease. *J. Biomol. Struct. Dyn.* **2000**, *17*, 787-797, <https://doi.org/10.1080/07391102.2000.10506568>.
137. de la Rica, R.; Matsui, H. Urease as a nanoreactor for growing crystalline ZnO nanoshells at room temperature. *Angew. Chem. Int. Ed.* **2008**, *47*, 1-4, <https://doi.org/10.1002/anie.200801181>.
138. Johnson, J.M.; Kinsinger, N.; Sun, C.; Li, D.; Kisailus, D. Urease-mediated room-temperature synthesis of nanocrystalline titanium dioxide. *J. Am. Chem. Soc.* **2012**, *134*, 13974-13977, <https://doi.org/10.1021/ja306884e>.
139. Sharma, B.; Mandani, S.; Sarma, T.K. Biogenic growth of alloys and core-shell nanostructures using urease as an at ambient conditions. *Sci. Rep.* **2013**, *3*, 2601, <https://doi.org/10.1038/srep02601>.
140. Shi, H.; Tan, L.; Du, Q.; Chen, X.; Li, L.; Liu, T.; Fu, C.; Liu, H.; Meng, X. Green synthesis of Fe₃O₄ nanoparticles with controlled morphologies using urease and their application in dye adsorption. *Dalton Trans.* **2014**, *43*, 12474-12479, <https://doi.org/10.1039/c4dt01161a>.
141. Emond, S.; Mondeil, S.; Jaziri, K.; André, I.; Monsan, P.; Remaud-Siméon, M.; Potocki-Véronèse, G. Cloning, purification and characterization of a thermostable amylosucrase from *Deinococcus geothermalis*. *FEMS Microbiol. Lett.* **2008**, *285*, 25-32, <https://doi.org/10.1111/j.1574-6968.2008.01204.x>.
142. Lim, M.-C.; Seo, D.-H.; Jung, J.-H.; Park, C.-S.; Kim, Y.-R. Enzymatic synthesis of amylose nanocomposite microbeads using amylosucrase from *Deinococcus geothermalis*. *RSC Adv.* **2014**, *4*, 26421-26424, <http://dx.doi.org/10.1039/C5RA02284C>.
143. Cobbette, C.S. Phytochelatins and their roles in heavy metal detoxification. *Plant Physiol.* **2000**, *123*, 825-832, <https://doi.org/10.1104/pp.123.3.825>.
144. Kang, S.H.; Bozhilov, K.N.; Myung, N.V.; Mulchandani, A.; Chen, W. Microbial synthesis of CdS nanocrystals in genetically engineered *E. coli*. *Ang. Chem. Intern. Ed.* **2008**, *47*, 5186-5189, <https://doi.org/10.1002/anie.200705806>.
145. Liu, F.; Kang, S.H.; Lee, Y.I.; Choa, Y.H.; Mulchandani, A.; Myung, N.V.; Chen, W. Enzyme mediated synthesis of phytochelatin-capped CdS nanocrystals. *Appl. Phys. Lett.* **2010**, *97*, 123703, <https://doi.org/10.1063/1.3485295>.
146. Park, T.J.; Lee, S.Y.; Heo, N.S.; Seo, T.S. *In vivo* synthesis of diverse metal nanoparticles by recombinant *Escherichia coli*. *Ang. Chem. Intern. Ed.* **2010**, *49*, 7019-7024, <https://doi.org/10.1002/anie.201001524>.
147. Oguri, T.; Schneider, B.; Reitzer, L. Cysteine catabolism and cysteine desulhydrase (CdsH/STM0458) in 3 *Salmonella enterica* serovar typhimurium. *J. Bacteriol.* **2012**, *194*, 4366-4376, <https://doi.org/10.1128/JB.00729-12>.
148. Bai, H.J.; Zhang, Z.M.; Guo, Y.; Yang, G.E. Biosynthesis of cadmium sulfide nanoparticles by photosynthetic bacteria *Rhodospseudomonas palustris*. *Coll. Surf B: Bioint.* **2009**, *70*, 142-146, <https://doi.org/10.1016/j.colsurfb.2008.12.025>.
149. Njålsson, R.; Norgren S. Physiological and pathological aspects of GSH metabolism. *Acta Paediatr.* **2005**, *4*, 132-137.
- Chen, Y.L.; Tuan, H.Y.; Tien, C.W.; Lo, W.H.; Liang, H.C.; Hu, Y.C. Augmented biosynthesis of cadmium sulfide nanoparticles by genetically engineered *Escherichia coli*. *Biotechnol Prog.* **2009**, *25*, 1260-1266, <https://doi.org/10.1002/btpr.199>.



© 2019 by the authors. This article is an open access article distributed under the terms and conditions of the Creative Commons Attribution (CC BY) license (<http://creativecommons.org/licenses/by/4.0/>).